Spatial Signaling in the Development and Function of Neural Connections

P. Read Montague, Joseph A. Gally, and Gerald M. Edelman

The Neurosciences Institute, New York, New York 10021

In the vertebrate central nervous system, afferent axons find their appropriate target structures under the influence of local environmental cues. In many target regions, appropriate patterns of activity in the afferents are also required to establish normal mappings between the source cells and the target region. Specific mappings arise in these targets because temporal contiguity in firing is somehow transformed into spatial contiguity of synaptic contacts. In this article, we propose a theory that utilizes the covariance of a transient diffusive signal produced at active synapses with the firing of presynaptic axon terminals to account for many of these activity-dependent features of vertebrate neuroanatomy. Computer simulations of the growth of axons within a three-dimensional volume of neural tissue reveal the generality of the proposed mechanism in accounting for the self-organization of a broad range of diverse neuroanatomical structures, including those in the cerebral cortex. The proposed mechanism is consistent with detailed anatomical and physiological data, and direct experimental tests of predictions of the theory are suggested.

The complex connectivity of the CNS of vertebrates is largely established during embryonic and early postnatal development. How this comes about remains one of the major unanswered questions in neurobiology. Within a remarkably brief period of time, large numbers of neurons differentiate, migrate to correct anatomical locations, and project processes that make thousands of contacts with appropriate targets (Cowan, 1978; Jacobson, 1978; Purves and Lichtman, 1985). For a number of reasons, it appears that the exact details of this connectivity cannot be solely the result of detailed genetic prespecification (Changeux and Danchin, 1976; Edelman, 1987). For example, it has been demonstrated that the CNS will adapt to environmental or experimental perturbations by forming abnormal but nevertheless functional neuroanatomy (Sperry, 1943a,b; Hubel and Wiesel, 1965, 1970; Van der Loos and Woolsey, 1973; Pettigrew, 1974; Rakic, 1976; Constantine-Paton and Law, 1978; Shatz and Stryker, 1978; LeVay et al., 1980; Frost and Metin, 1985; Sur et al., 1988). Moreover, experimental data suggest that the epigenetic development of specific connectivity in the CNS initially requires a series of local cues that permit axons to reach the appropriate target regions (Bonhoeffer and Huff, 1985; Dodd and Jessel, 1988; Stuermer, 1988; Harris, 1989; Harris and Holt, 1990; Sretavan, 1990).

In many regions, after reaching the target area, activity-dependent signals are then required for these axons to establish appropriate, refined connections (for reviews, see Sherman and Spear, 1982; Udin and Fawcett, 1988; Constantine-Paton et al., 1990). Many elegant experiments over the last 25 years have shown that specific temporal patterns of neural activity are required to permit appropriate and specific spatial patterns of synaptic connections to form during development (Hubel and Wiesel, 1965, 1970; Rakic, 1976; Hubel et al., 1977; Constantine-Paton and Law, 1978; Shatz and Stryker, 1978, 1988; Schmidt and Eisele, 1985; Dubin et al., 1986; Stryker and Harris, 1986; Reiter and Stryker, 1988). For example, mappings from peripheral sensory structures to central structures in the thalamus, cerebral cortex, and tectum all require appropriate specific patterns of neural activity to form, to function normally, and to reorganize after perturbations (thalamus: Dubin et al., 1986; Garraghty et al., 1988; Shatz and Stryker, 1988; Sretavan et al., 1988; cerebral cortex: Hubel and Wiesel, 1965, 1970; Van

der Loos and Woolsey, 1973; Woolsey and Wann, 1976; Hubel et al., 1977; Van der Loos and Dorfl, 1978; Rakic, 1981; Stryker and Harris, 1986; Dawson and Killackey, 1987; Swindale, 1988; Metin and Frost, 1989; tectum: Meyer, 1982; Reh and Constantine-Paton, 1985; Schmidt and Eisele, 1985; Cook, 1987; reorganization of mappings: Merzenich et al., 1985; Clark et al., 1988; Kaas et al., 1990).

The results of all these experiments raise the possibility that there is some general mechanism by which patterns of neural activity guide the development of neural connectivity. Two generalizations have emerged from the study of such activity-dependent processes: (1) In a local volume of neural tissue, axon terminals that tend to fire together terminate into common spatial domains, and axons that tend not to fire together segregate into separate spatial domains. In other words, within a population of axons innervating a common local region, temporal contiguity in firing is somehow transformed into spatial contiguity of synaptic contacts. (2) Some kind of postsynaptic response is necessary for synaptic plasticity and appropriate segregation to occur (Rauschecker and Singer, 1979; Cline et al., 1987; Fregnac and Imbert, 1984; Reiter et al., 1986; Kleinschmidt et al., 1987; Fregnac et al., 1988; Reiter and Stryker, 1988; Bear et al., 1990; Schmidt, 1990). Evidence suggests that, though it is not necessary that the postsynaptic cell actually fire to induce synaptic plasticity appropriate for segregation, local responses within the dendritic arbors of these cells are required (Reiter and Stryker, 1988; Bear et al., 1990). Moreover, various experiments have demonstrated that, in some systems, activation of NMDA receptors is required for such segregation to occur (Cline et al., 1987; Artola and Singer, 1987, 1990; Kleinschmidt et al., 1987; Scherer and Udin, 1989; Bear et al., 1990; Cline and Constantine-Paton, 1990; Schmidt, 1990).

Given that axonal terminals segregate into separate spatial domains based upon their activity patterns, some form of spatial signaling must occur that effectively communicates the temporal patterns of synaptic activity in a local volume to the presynaptic terminals innervating that volume. If this were not the case, axon terminals could not be excluded from the local volume on the basis of their firing patterns.

In this article, we present a theory in which we propose that spatial signaling occurs via a short-lived, rapidly diffusing substance. This mechanism appears to be sufficient to generate a variety of anatomical structures similar to those found in the vertebrate neocortex and thalamus. We compare this mechanism to previously proposed models and then provide detailed demonstrations of its efficacy by means of computer simulations of neuropil development.

Previous Proposals

Two mechanisms of spatial signaling have previously been explicitly or implicitly presumed to operate; alone or in combination, these could communicate presynaptic activity patterns throughout a local target region of neural tissue.

First, the patterns of activity in the afferent axons might be communicated throughout the region by axons originating in postsynaptic cells located in the target region (Fig. 1*A*; Pearson et al., 1987). Competition among the axonal terminals could then be mediated by signals produced by and communicated within individual dendritic arbors (heterosynaptic signals). Those synapses that fired at the right time in the right place would be stabilized, and those that did not would be removed in a manner consistent with a form of eliminative selection (Changeux et al., 1973; Changeux and Danchin, 1976; discussed in Edelman, 1987). By utilizing synchronous activity in axon collaterals, this model permits communication between distinct dendritic arbors that are nonoverlapping and are not necessarily covered by the same afferent axonal arbors (Finkel and Edelman, 1987). It is important to note that this model requires the firing of the postsynaptic neurons in order to effect spatial signaling. Recent work suggests, however, that production of action potentials by postsynaptic cells may not be required in some systems for appropriate segregation of afferents during development (Rauschecker and Singer, 1979; Fregnac and Imbert, 1984; Cline et al., 1987; Kleinschmidt et al., 1987; Fregnac et al., 1988; Reiter and Stryker, 1988; Bear et al., 1990; Schmidt, 1990).

A second spatial signaling mechanism is as follows: all axons entering a region could branch so exuberantly and indiscriminately that each afferent axon would tend to make synapses onto most or all target dendritic arbors in the region (Fig. 1*B*). The firing patterns of presynaptic fibers could then be communicated throughout the region by the exuberance and overlap of axonal arbors. As in the first mechanism, synaptic competition is mediated within dendritic arbors.

The development of certain neural regions presents difficulties for these two mechanisms. First, neural regions without sufficient initial exuberance and overlap of the afferent axons are not explained by the mechanism in Figure 1*B*. In the mammalian cerebral cortex, for example, the formation of clustered connections between local domains that have similar orientation selectivity does not develop simply from the pruning of initially exuberant and overlapping axons. Rather, a combination of sprouting and retraction results in this pattern of linkages in the cortex (Callaway and Katz, 1990, 1991). This combination of both selective sprouting and retraction has also been reported in a number of structures, including the thalamus (Sretavan and Shatz, 1986) and the geniculocortical projection to area 18 (Friedlander and Martin, 1989).

Other regions provide difficulties for the mechanisms in Figure 1, *A* and *B*. These regions include those with sparse or ineffective local excitatory connections between projection neurons, for example, the thalamus (Jones, 1985). If distinct afferent axons transmitting different patterns of action potentials must synapse on the same postsynaptic cell in order to "sense" each other's firing pattern, then a severe sam-

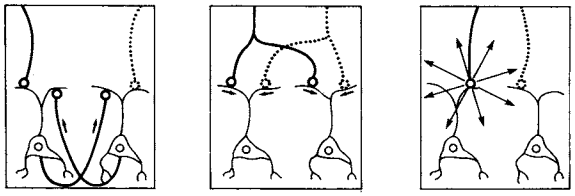

Figure 1. Possible mechanisms by which patterns of afferent activity could be distributed among populations of postsynaptic cells. *A*, Different afferent axons (*solid* and *broken lines* entering from *above*) make contact with dendrites of different target neurons. Action potentials in axons of postsynaptic cells (*arrows*) spread afferent firing patterns throughout the local volume. Competition among different activity patterns occurs within individual dendritic arbors and results in the strengthening of synapses that fire together and the weakening and potential disruption of others. *B*, As in *A*, except that axon collaterals originating in postsynaptic cells are absent, sparse, or ineffective. Because postsynaptic cells are not synaptically interconnected, the spread of the signal (*arrows*) among different cells must be mediated by the overlap of the *afferent* axonal arbors. *C*, As in *A*, except that active synapses release signal (*arrows*) in the form of a short-lived substance that diffuses throughout the local volume. In this mechanism, the postsynaptic response is integrated in extracellular space as well as within neurons. Synapses that are close together in space and fire in synchrony will be strengthened, even if they are not anatomically linked.

Table 1
Rules for changes in synaptic strength

	High [*x*]	Low [*x*]
Presynaptic terminal firing	increase	decrease
Presynaptic terminal not firing	decrease	no change

[*x*], concentration of diffusible signal. High [*x*] and low [*x*] represent values of [*x*] that are above or below thresholds for potentiation or depression. See Appendix 1 for these thresholds.

pling problem is encountered. The data suggest that somehow the afferents are removed from volumes that are defined by the activity patterns. In the absence of some other signaling mechanism, how are the firing patterns on one dendritic arbor made accessible to the firing patterns impinging on another distinct dendritic arbor if the local excitatory collaterals do not provide the spatial signaling between distinct dendritic arbors in the region? Even though one or both of these mechanisms may work in particular brain regions, a more general mechanism appears to be required. The mechanism we propose involves spatial signaling via a rapidly diffusible substance released at active synapses.

It should be noted that we point out these potential problems with previous models in order to identify them, not necessarily to discard them. As no *argument* can rule out these models, we simply assert that they have difficulties and have not yet proven to be sufficient to explain all of the observations associated with the development of specific connections in the cerebral cortex and thalamus.

A Short-lived Diffusible Substance as a Spatial Signal

According to the present proposal, a short-lived substance is released at active synapses and acts as a transient spatial signal (Fig. 1*C*; Gally et al., 1990). This substance moves out into the immediately surrounding extracellular space and affects synaptic contacts throughout the local region. Rapid temporal fluctuations in the presynaptic firing patterns are transformed into rapid spatiotemporal fluctuations in the substance concentration. Those synapses that depolarize when the concentration of this compound in the surrounding volume is high are strengthened, and those that do not depolarize at such times, or that depolarize when the concentration of the substance is low, are weakened or broken (Table 1; see also "Detailed Theory and Computer Simulation Methods," below). Acting against a background of axonal growth during development, this scheme for synaptic stabilization allows transient spatial patterns of substance concentration to transform temporally correlated firing patterns into spatially correlated patterns of stabilized synaptic contacts.

The proposed mechanism places constraints on the spatiotemporal properties of the diffusible spatial signal. In response to afferent activity in a common volume of tissue, production and removal of the substance must be sufficiently rapid to allow different temporal patterns of afferent activity to be distinguished. If the temporal variation in the substance concentration did not reliably follow afferent activity patterns, then different patterns would not be distinguished as such and would not be sufficient to direct the appropriate segregation of the afferent terminals. This last requirement rules out substances that are produced, act, or are degraded too slowly relative to the relevant temporal patterns of activity known to direct segregation in a particular region.

We emphasize that the signal substance acts throughout a local *volume* and is not confined to specific cells or dendrites. It does not act directly to affect gene expression or to alter cell proliferation, differentiation, migration, or survival. It would therefore be misleading to refer to this substance as either a trophic, tropic, or chemotactic factor, even though the indirect consequences of the function of the substance might mimic the effect of such factors. The signal would be produced at temporal and spatial scales that constantly changed during the growth and segregation of the afferent terminals, because the sources of substance production (active synaptic contacts) can appear (sprouting), disappear (synapse removal), and move (growth and new branch formation).

There are two additional properties of the proposed mechanism that should be noted (Fig. 2). The first, self-scaling (Fig. 2*A–C*), is particularly important for the formation and refinement of topographic mappings (see Fig. 6). During the initial innervation of a target region (Fig. 2*A*), the axons form sparse, transient contacts that produce low levels of the substance. At this time, fluctuations in substance concentration at small spatial and temporal scales are too close to the average background levels to cause stable changes in synaptic strengths and are not sufficient to guide branching at these smaller scales.

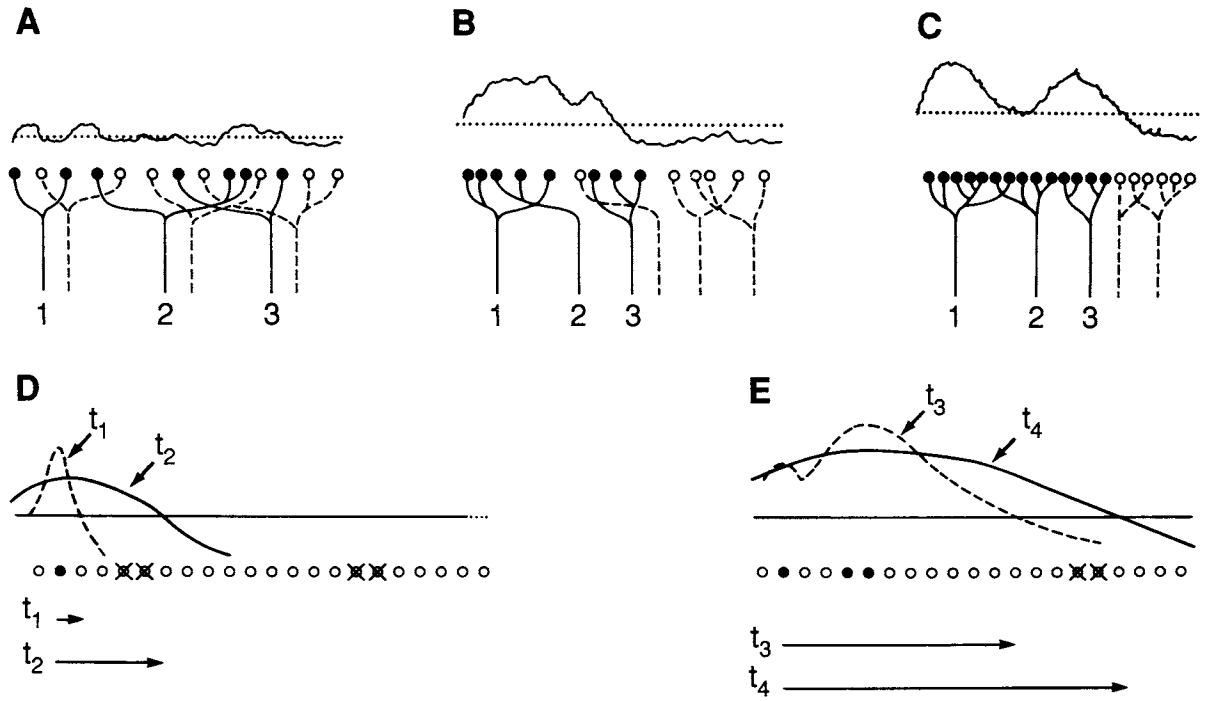

Figure 2. Self-scaling of diffusible signal. For simplicity, a one-dimensional array of synaptic contacts is shown. The *solid* and *broken* afferent axons serve two different sources (e.g., right and left eyes) that compete for postsynaptic targets. In *A–C*, the *dotted line* represents the average background level of the postulated signaling substance throughout the region, and the *solid line* represents its concentration throughout the region due to the firing of presynaptic *axons 1* and *3*. During the early innervation of the target (*A*), synaptic contacts are weak and dispersed. The covariance of presynaptic activity and substance concentration is insufficient to mediate synaptic plasticity appropriate for segregation of the arbors. Local branching and synapse formation occurs until axons serving a single afferent source can cooperate to yield sufficient covariance of source-specific firing and substance concentration. This cooperativity results in the formation of crude source-specific zones as illustrated in *B*. Subsequently, smaller-scale correlations of presynaptic activity due to the correlated firing of neighboring neurons in each source (e.g., retinal neighborhoods) become sufficient to effect the further refinement of the afferent terminals shown in *C*. *D* and *E*, Saltation of synaptic strength changes due to cooperativity between active correlated synapses. Synapses are shown as a one-dimensional array of *circles* below a horizontal *solid line* representing the threshold concentration of signal substance needed to strengthen active synapses. In *D*, a single active synapse (*solid circle*) is strong enough to produce signal, whose concentrations at times t_1 and t_2 are shown by the *broken* and *solid curves*, respectively. The activity of synapses marked with *X*s is correlated with the source synapse, but their synaptic strength is initially insufficient to produce substance. At time t_2, due to diffusion and additional production of substance, suprathreshold levels exist at additional correlated synapses, and they become active sources (*solid circles*, as shown in *E*). In *E*, this cooperative interaction has resulted in a synergistic increase in the concentration and spread of the substance at time t_3 (*broken curve*). At the next time point (t_4), the signal has spread such that even more distant synapses can be strengthened, conferring a kind of saltation to the changes in synaptic strength. These cooperative effects on the lengths of diffusive linking (indicated as *arrows* beneath the synapses) permit changes in synaptic strength to move through tissue faster than the actual diffusion of substance.

Under the influence of specific temporal patterns of firing in a region, subsequent branching and new synapse formation cause the average background level of substance to increase. This selective addition of synapses in appropriate local volumes also permits the stable covariance of presynaptic firing and substance concentration to occur. The correlated fluctuations in firing and substance levels are largest at coarse spatial and temporal scales. Segregated structures based on gross differences in input activity patterns, such as eye-specific laminae or crude somatotopic zones, could be formed by such rough mapping (Fig. 2*B*). As synapses begin to stabilize, however, the scales at which the covariance differs significantly from background diminish in size, and the developing map is able to respond to increasingly fine differences among spatiotemporal patterns of input activity (Fig. 2*C*; see also Fig. 7).

A second important property is a kind of saltation effect illustrated and explained in Figure 2, *D* and *E*. This effect allows changes in synaptic strength in one local volume to be communicated to another noncontiguous local volume at a rate much faster than that predicted for the actual diffusion of a substance through the intervening distance.

Detailed Theory and Computer Simulation Methods

Simulations were carried out to examine how this proposed mechanism guides the growth of axons into a region containing potential synaptic targets. The simulations were run on an NCUBE/10 parallel computer using the developmental network simulator (dns) developed and written by one of us (P.R.M.) from a minimal version of the cortical network simulator (cns) of Reeke (Reeke et al., 1990).

Conceptually, the model used to examine the theory is straightforward and depends on four assumptions: (1) The postsynaptic voltage at each synaptic contact is proportional to the presynaptic activity times the synaptic strength. (2) Cell firing rate or the probability that the cell fires is a weighted sum of the voltages at each synaptic site located on its dendritic arbor. The key assumptions are that (3) the hypothesized substance is produced at a rate proportional to the postsynaptic voltage, and (4) the synaptic strength at each synaptic site changes according to

the covariance of the presynaptic activity and local substance concentration.

Axonal Growth and Connectivity

We simulated the growth of axons into a three-dimensional recipient region containing cells with dendrites (Fig. 3). The axons can originate in external sensory sheets or from cells located within the simulated volume. These fibers can actively move throughout the volume independent of their electrical activity. As the axons grow and sprout branches, synapses can be made and broken throughout the region, and these contacts are strengthened or weakened depending upon patterns of axonal activity and transient substance levels, that is, according to the synaptic rules described in Table 1.

In the simulations, postsynaptic cells with dendrites preexist within the three-dimensional volume, and these provide a fixed number of potential postsynaptic sites. Although the geometry of dendritic arbors was explicitly modeled, the structure of these arbors did not change during the course of any simulation. All synaptic contacts that were potential sources of production of the spatial signal were modeled as excitatory. In some simulations, the growth of axons originating in inhibitory cells was also included, but these inhibitory contacts were not sources of substance production.

In the computer model, the behavior of the simulated growth cones is assumed to be autonomous, so that the growing tips of the same axonal arbor have only their times of depolarization in common and do not otherwise detect their common ancestry. Growth of axons throughout the simulated volume occurs as follows: an empty postsynaptic site allows the ingrowth of an axonal terminal from a surrounding neighborhood in a fashion that is independent of the current structure of the axon or any property of the source cell.

At every time step, each unoccupied postsynaptic site on a dendrite randomly chooses another postsynaptic site in its neighborhood and accepts, with a preset probability (0.2–0.3; denoted p_{acc}), a branch from the presynaptic axonal terminal that innervates that chosen postsynaptic site (i.e., randomized local sprouting or growth). If no presynaptic terminal occupies the chosen site or if the chosen site is not accepted, then the empty site remains empty. In selecting a presynaptic terminal from this neighborhood, distances along each axis of a coordinate system centered on the empty site are chosen in accordance with Gaussian distributions. Thus, the average growth rate of any axon is a function of the preset probability of accepting a chosen site, the regional synaptic activity, and the availability of postsynaptic sites.

If the synaptic strength of an established synapse drops below a preset value, the connection is broken and that branch is retracted into the parent branch. The specific details of arbor structure therefore do not result from growth rules for axons, but instead reflect statistical relationships among a number of variables, which include regional firing patterns, growth velocity, crowding effects, dendritic geometry, and a limited number of potential postsynaptic sites.

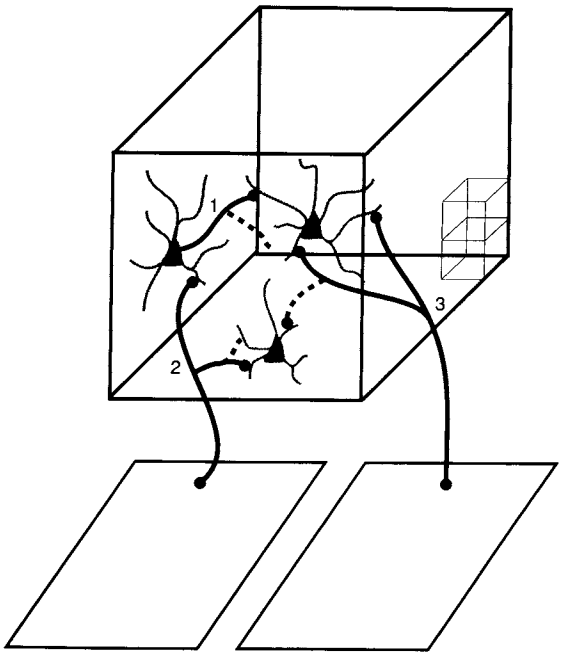

Figure 3. Generalized diagram of neural connectivity within the simulated neural tissue. Sensory sheets are composed of cells distributed within a two-dimensional array. These sheets project axons (*2* and *3*) into the rectangular volume containing the dendritic arbors of target cells. In some simulations, these target cells also project axons (*1*) that make synaptic contacts with dendritic arbors in this same volume. To simulate axonal growth, empty synaptic target sites select contacts from axons in the surrounding space. New axonal branches formed in this process are indicated by *broken lines*. (In Figs. 4–8, only new axonal sprouts are illustrated; cells, dendritic arbors, and initial axonal arbors are not shown). In all the simulations, dendrites arborize randomly around the cell of origin with an explicit spatial structure that approximates either spherical or cylindrical symmetry. To calculate the distribution of the spatial signal within the neural tissue at each time step, the entire tissue was divided into *cubic compartments* (indicated at the *back* of the volume). The concentration of signal substance within each compartment is uniform; diffusion occurs between compartments that share a face. Initial connections between a sensory sheet and targets in the simulated volume are assigned either diffusely throughout the volume or topographically, having a Gaussian divergence of the spatial extent of each arbor. The degree of this divergence and the fraction of synaptic target sites filled initially were varied in different simulations. Other parameters specified at the start of each simulation were the mean and variance of synaptic efficacy, whether the synapses from any source were excitatory or inhibitory, and the amount of signal substance that each produced. For all simulations presented, the neuropil is presented with the reader looking down the z-axis, and the branches of the axons are drawn from each sprout site to the site where the sprout made a contact that was stabilized. When a contact breaks, this line is retracted into the parent branch and is not drawn on the next cycle of the simulation. Intensity coding is used to distinguish front from back.

Synaptic Voltage

The postsynaptic voltage, v_i, at each synaptic contact is

$$v_i(t) = k_i \cdot c_{ij}(t) \cdot (s_j(t) - \theta_e),$$

where i indexes the postsynaptic site, and j indexes the presynaptic axonal terminal. $s_j(t)$ is the probability that presynaptic terminal j fires at time t where $s_j(t) \in (0,1)$, and θ_e is a fixed excitatory threshold set at 0.25 for all simulations reported in this article. The voltage at each synaptic site does not decay, but takes on instantaneous values at each iteration; however,

the persistence of the substance serves to carry information about local activity from preceding time steps. The difference $(s_j(t) - \theta_e)$ is not allowed to be negative. $c_{ij}(t)$ is the synaptic strength between presynaptic terminal j and postsynaptic site i at time t, and k_i is a positive scale factor for synaptic site i. For inhibitory synapses, $c_{ij} \in [-1,0)$, and for excitatory synapses, $c_{ij} \in (0,1]$.

Cell Firing

The probability of firing of a single cell is calculated as a weighted average of the activity of all synapses on the dendritic arbor of the cell. The probability that cell i fires (s_i) is given by $s_i = 5.5 \cdot \sum_j v_j$, where j ranges over all synapses onto cell i. s_i was clipped at 1.0.

Diffusion

We modeled tissue space explicitly as a collection of cubic compartments. The flux of the substance between compartments was assumed to be a linear function of the concentration differences between compartments that share a face. Destruction of the substance occurs throughout the simulated volume at a constant rate κ. The substance concentration at a location $\mathbf{x}$ and time t, denoted $u(\mathbf{x}, t)$, can be described by a diffusion equation with a first-order decay term,

$$u_t(\mathbf{x}, t) = D \cdot \nabla^2 u(\mathbf{x}, t) - \kappa \cdot u(\mathbf{x}, t) + p(\mathbf{x}, t),$$

where ∇^2 is the Laplacian operator, D is the diffusion constant, $u_t(\mathbf{x}, t)$ is the time derivative of $u(\mathbf{x}, t)$, and $p(\mathbf{x}, t)$ is the instantaneous production of substance at location $\mathbf{x}$ and time t. In the simulations, the concentration of substance in the compartment containing synaptic site i is denoted by u_i. The relationship between this diffusion equation and the compartmental simulation is discussed in Appendix 2.

Synaptic Strength Changes

The potentiation and depression of synaptic strengths in the simulation were divided into separate components. This treatment is consistent with the assumption that these processes would be mediated by different biochemical mechanisms and thus have related but separate actions (Artola et al., 1990; Goldman et al., 1990). At each synapse, synaptic strength is increased or decreased as a function of the covariance between the substance concentration and the presynaptic firing. The contingencies for synaptic strength change are listed in Table 1, and the specific details of synaptic change are described in Appendix 1.

In the simulations, changes in synaptic strengths and the growth of axons occur more slowly than the rate at which the substance is produced and removed from a locale. The value of $u_i(t)$ is the only signal linking activity at different synaptic sites, and no intracellular signal is transmitted within dendritic arbors. Heterosynaptic effects are thus the consequence of the transmission of signals directly through the tissue rather than within dendritic arbors (Lynch et al., 1977; Finkel and Edelman, 1987; White et al., 1988, 1990).

A simple calculation illustrates the ability of the proposed mechanism to resolve temporal patterns of presynaptic activity in a local region. Suppose, for example, that the synapses are homogeneously distributed in a spherical volume with a radius of 100 μm, approximately the radius of a whisker barrel in the rodent somatosensory cortex. A synchronous burst of activity in these synapses would rapidly produce a uniform concentration, u_0, throughout the sphere faster than other effects such as synaptic change or axonal sprouting.

The time required for the initial concentration to be approximately halved by diffusion of the substance into the surrounding tissue is

$$t = a^2/(4 \cdot D),$$

where t is time, D is the diffusion constant, and a is the radius of the sphere (Crank, 1955). If the threshold for potentiation, T_2, is equal to $u_0/2$ (see Appendix 1), a second population of nonproducing synapses would have to fire within this time t in order to be potentiated. These times are approximately 1 sec, 3 sec, and 35 sec, respectively, for a diatomic gas (carbon dioxide, 1.92; nitric oxide, 2.60), amino acid (valine, 0.83), and protein (hemoglobin, 0.069; ovalbumin, 0.078). The diffusion constants listed above are expressed in $10^{-5} \cdot cm^2 \cdot sec^{-1}$ at 25°C (Cussler, 1984).

These simple calculations indicate that, for those regions of the brain in which afferent activity patterns fluctuate at short time scales (20–500 msec), even rapidly diffusing substances would have to be removed or destroyed by some means other than simple diffusion. Otherwise, spurious correlations with axonal terminals firing at later times would result from the persistence of the substance. Such spurious correlations would disrupt appropriate changes in synaptic strength. The proposed mechanism therefore would fail to resolve distinct temporal patterns in the afferent terminals, and aberrant spatial patterns of synaptic contacts would form in a region.

Results

We have modeled a variety of situations to examine how the proposed mechanism would actually direct the growth of axonal arbors in regions containing various target dendritic arbors.

Development and Perturbation of Whisker Barrels and Barreloids

Sensory neurons innervating rodent vibrissae terminate in segregated neural structures in the trigeminal nucleus (Belford and Killackey, 1979). These in turn innervate segregated structures in the thalamus called barreloids. Barreloids innervate distinct structures in the somatosensory cortex called whisker barrels (Killackey, 1973; Woolsey et al., 1975). This aggregation of axonal terminal arbors into whisker-specific units at each of these stages from sensory nerve to cerebral

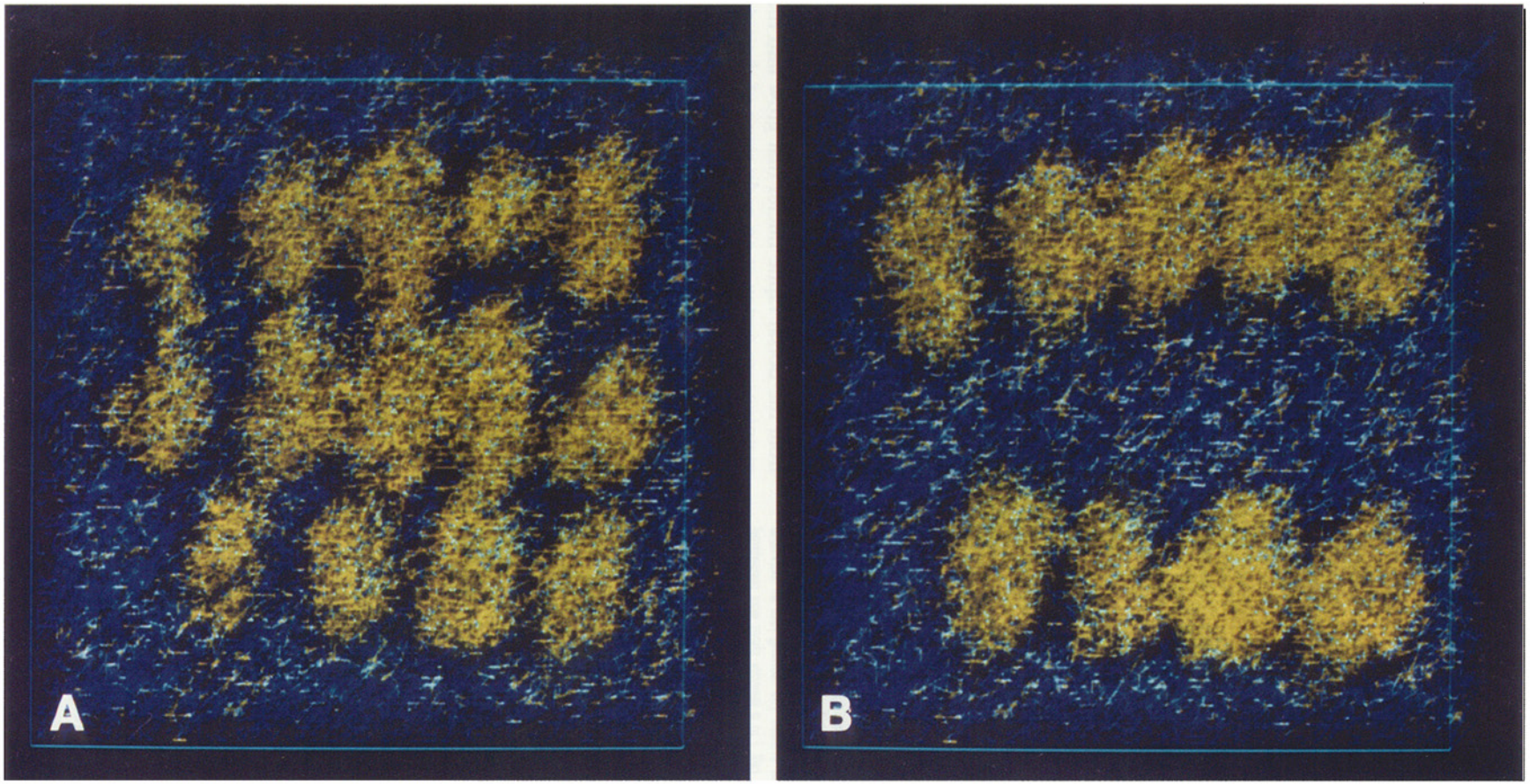

Figure 4. Simulated formation of barreloids. Axons shown in *yellow* arise from a 64 × 64 sensory sheet composed of 4096 excitatory cells. This sensory sheet projects with loose topography into the simulated three-dimensional region. The initial connections from the sensory sheet into the three-dimensional volume enter topographically and display randomized variance along x-, y-, and z-axes with $\sigma_x = \sigma_y = 1.0$. In this simulation, 95% of the synaptic contacts from an individual axon from the sensory sheet could cover up to 7% of the length along the x- and y-axes and 100% along the z-axis. Only 20% of all possible postsynaptic sites are initially filled ($f = 0.20$). The pattern of stimulation was a random series of short bursts of activity from 13 spatially distinct loci. Each locus (whisker) was represented by 24 cells in a 6 × 4 rectangle in the sensory sheet. Three loci were made coactive for two cycles, followed by two cycles of rest. The set of three loci chosen was randomized so that no two loci were coactive for successive rounds of stimulation. Axons shown in *blue* originated in a separate 64 × 64 sensory sheet; the activity of these cells was randomized (drawn from a Gaussian distribution with mean = 0.5 and SD = 0.25) and did not correlate with the whisker stimulation. Both the *yellow*- and *blue*-labeled fibers made excitatory synapses in the neuropil and were sources of signal substance. *A*, Three-dimensional neuropil after 77 cycles of the simulation. Axonal arbors of fibers serving whiskers (*yellow*) have formed into barreloid-like structures. When excitatory collaterals were included in related simulations, similar but more spherical structures formed. *B*, The middle row of whiskers was made inactive (plucked) before the sensory sheet was stimulated. All other parameters were the same as in *A*. The *light blue* fibers are a graphical artifact due to overlap of *yellow* and *blue* fibers in the immediate foreground. $D = 0.13$; DR = 0.70; IC = 100.0; PR = 35.0; $T_1 = 20.0$, $T_2 = 40.0$, $T_3 = 100.0$; $NC_x = 32$, $NC_y = 32$; $NC_z = 32$; $p_{acc} = 0.4$; $c_{tck} = 0.2$; $n_x = 1.0$, $n_y = 1.0$, $n_z = 1.0$; eight layers of synaptic sites, each 100 × 100 − NS = 80,000; $\delta = 0.04$.

Table 2
Abbreviations and parameters used in Figures 4–8

Abbreviation	Definition
D	Effective diffusion or coupling constant for the substance
DR	Destruction rate for substance
PR	Production rate for substance
IC	Initial concentration of substance at the beginning of a simulation
T_1, T_2, T_3	Substance concentration thresholds for potentiation and depression. These are defined in text, and their interaction is discussed in Appendix 2.
NC_x, NC_y, NC_z	Number of compartments along x-, y-, and z-axes, respectively. It must be noted that the layers of potential postsynaptic sites were *always* positioned within the simulated tissue space to maintain synaptic densities as isotropic as possible; see Appendix 2.
NS	Total number of potential postsynaptic sites for the simulation.

The synaptic strengths of initial synaptic connections were drawn from a Gaussian distribution with mean = 0.39 and SD = 0.13. The synaptic strengths of newly sprouted synapses were drawn from the same distribution. For specifying the initial connectivity of the axons and the potential spatial spread of the dendrites, the standard deviations of the spread along the x- and y-axes are denoted σ_x and σ_y (Appendix 2). Throughout a region potentially covered by an axon terminal or dendrite, the fraction of sites actually filled is denoted by f. A description detailing the initial assignment of topographic input is given in Appendix 2. Parameters associated with the making and breaking of synapses are as follows: p_{acc}, probability that an unoccupied postsynaptic site accepts a branch from the axon terminal innervating a randomly chosen postsynaptic site in a stochastically determined neighborhood of the postsynaptic site. n_x, n_y, n_z, standard deviations of Gaussian distributions along x-, y- and z-axes and centered on a postsynaptic site that define the stochastic neighborhood from which an afferent axon can sprout into the site during the next time step; c_{brk}, synaptic strength threshold for breaking a contact between an afferent axon and a postsynaptic site. Once the synaptic strength of the connection drops below this threshold, the contact is broken and the branch is retracted into the parent branch. The learning rate at individual synapses is denoted by δ (Appendix 1). A cell i in a sensory sheet was considered active at time t if $s_i(t) > 0$.

cortex has been shown to depend on the temporal patterns of sensory neural activity transmitted along this pathway. If a whisker is removed from a newborn animal, the corresponding structures in the CNS do not develop, and the remaining structures reorganize in a manner that appropriately reflects the patterns of activity in the input (Van der Loos and Woolsey, 1973; Woolsey and Wann, 1976; Belford and Killackey, 1979; Killackey and Belford, 1979; Durham and Woolsey, 1984; Dawson and Killackey, 1987; Jensen and Killackey, 1987a,b).

To simulate the development of barreloid-like structures, input from whisker afferents was modeled as a cell layer that projected in a loosely topographic fashion into the simulated neuropil (Fig. 4). Excitatory axon collaterals originating in the recipient region were not present in barreloid formation, but the development of the whisker barrels included these collaterals (see Fig. 4 caption and Table 2).

The simulated pattern of activity in whisker afferents consisted of random series of short bursts of high activity from 13 distinct loci. In the present simulations, activity in any pair of whiskers was uncorrelated. Afferent axonal terminals arising from common regions of high activity grow, branch, and aggregate into tight structures that are spatially distinct from those generated by axons firing at other times (Fig. 4*A*). Although the effect can be complicated, the primary determinant of the formation of these barreloid structures is the statistics of the temporal correlations in the simulated whisker afferents as they interact with the developing arbor sizes [see Miller et al. (1989) for a linear analysis of the interaction of correlations in input activity and axonal arbor sizes]. In addition to the simulated whisker input, axons from cells that fire in an uncorrelated fashion were also present (Fig. 4*A*, blue fibers), and these were squeezed into narrow volumes between the barreloids and whisker barrels.

The experimental perturbation of sensory input was mimicked in two ways: (1) deleting input from a row of cells in the sensory sheet to simulate plucking a row of whiskers before significant ingrowth of afferents and (2) firing a row of afferents in a temporally correlated fashion so that the pattern of input activity is similar to that obtained by taping adjacent whiskers in an animal. The first perturbation is illustrated in Figure 4*B* and gives rise to structures similar to those seen *in vivo* in response to similar manipulations (Dawson and Killackey, 1987; Rhoades et al., 1990). The second perturbation is not shown but resulted in the fusion of those whisker barrels whose activity was correlated.

Organization of Nontopographic Input

The axonal arbors of cells that are *not* organized topographically in sensory sheets can also become anatomically segregated in CNS structures. It has been demonstrated, for example, that serotonergic axons from the dorsal raphe nuclei that grow into the somatosensory cortex at an early stage of their development form patterns (somatotopic mappings) similar to those of the thalamocortical axons (Rhoades et al., 1990). This is noteworthy because there is no somatotopic map in the dorsal raphe nuclei. A spatial signal of the sort we are proposing provides a possible mechanism for the spatial organization of these nontopographic fibers.

In Figure 5, the serotonergic axonal input is modeled as a population of axons that are initially *nontopographically* distributed throughout the simulated neuropil (yellow fibers). As before, the topographic afferents (red fibers) originate in a sensory sheet and provide the punctate stimuli needed to generate the barreloid or whisker barrel structures. Firing of *all* of the nontopographic serotonergic axons is temporally correlated with the firing of *each* punctate stimulus that stimulates whisker stimulation. This temporal correlation in firing would be expected with the general arousal and midbrain firing associated with whisker stimulation. Under these conditions, as shown in Figure 5, the spatial signal generated at the thalamic terminals (red fibers) induces both topographic (red fibers) and nontopographic (yellow fibers) afferents to segregate into barreloid-like structures. Although certain specific features differ, this effect is essentially similar to the development of appropriate registration of topography by the cholinergic projection from the nucleus isthmi to the contralateral optic tectum in *Xenopus laevis* (Scherer and Udin, 1989; Udin and Scherer, 1990).

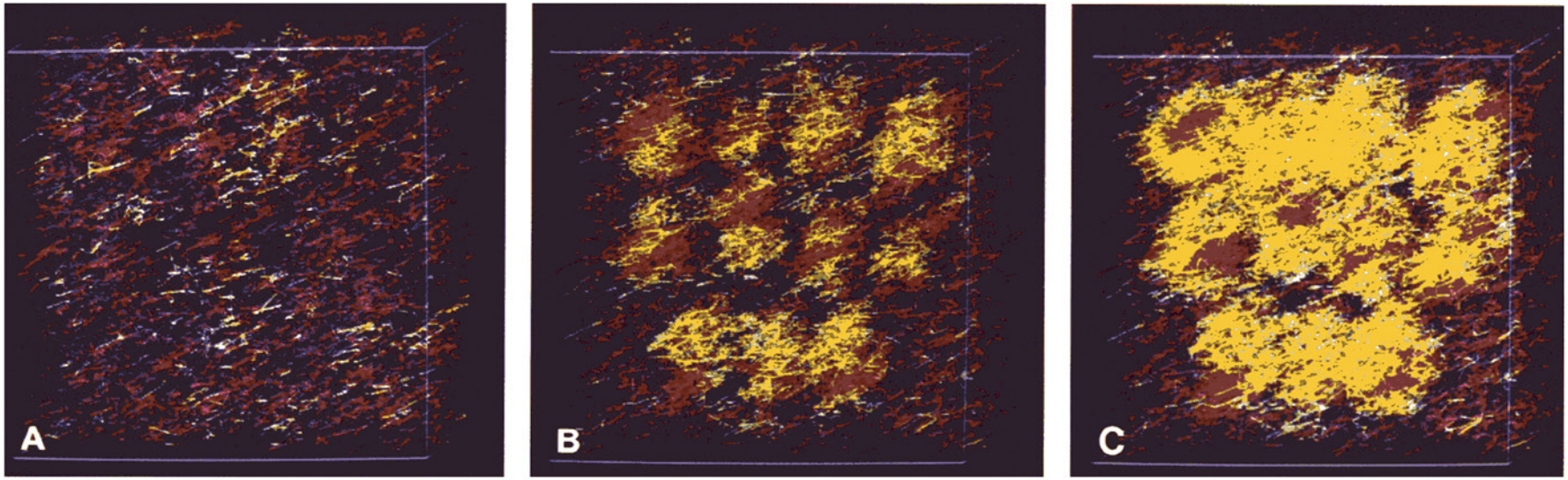

Figure 5. Organization of diffuse projections by temporal correlations. The simulation was the same as in Figure 4 except that an additional population of 4096 axons were allowed to grow into the simulated tissue space from a third 64 × 64 layer of cells. *Red* axons originated in a topographically projecting sensory sheet (same initial connectivity as in Fig. 4); *yellow* and *blue* axons projected into the simulated volume with no topography and were initially assigned to uniformly distributed synaptic sites. As in Figure 4, only 20% ($f = 0.20$) of the postsynaptic sites were initially filled, but in this case, the filled sites were evenly distributed among the three sources of afferent fibers into the simulated tissue space. Thus, the density of contacts from the topographic input was less than that in Figure 4. Stimulation of the topographic input was identical to that in Figure 4. Firing of cells providing *diffuse* input (*yellow* fibers) was *temporally* correlated with activity occurring in the topographic input. Synapses from the diffuse projections *did not* produce the spatial signal, but they were strengthened or weakened according to the covariance of their firing and the concentration of the signal. A–C show the growth of axons at cycles 5, 65, and 177, respectively. As in Figure 4, barreloid-like structures are formed. In addition, the temporal correlation of the firing of the diffuse projection causes the diffuse axons to sprout densely in a corresponding pattern. If the correlation between the firing of the diffuse fibers and the topographic fibers is disrupted or the substance was not produced, then the diffuse fibers do not organize into barreloid structures. $D = 0.13$; DR = 0.70; IC = 100.0; PR = 80.0; $T_1 = 20.0$, $T_2 = 40.0$, $T_3 = 100.0$; $NC_x = 32$, $NC_y = 32$, $NC_z = 32$; $p_{acc} = 0.4$; $c_{tck} = 0.2$; $n_x = 1.0$, $n_y = 1.0$, $n_z = 1.0$; eight layers of synaptic sites, each 100 × 100 − NS = 80,000; $\delta = 0.04$.

Development of Ocular Dominance Patches and Retinotopy

In many higher vertebrates, afferents carrying signals from both eyes initially project axons that map topographically into common regions in the thalamus and the cerebral cortex. By some unknown mechanism, the afferents from the two eyes apparently compete for regions of neural tissue. As a result of this competition, those axons receiving input from one eye tend to terminate within regions different from those innervated by the other eye (Hubel and Wiesel, 1965).

A number of abstract models have been proposed to account for the general shape and periodicity of these structures (von der Malsburg and Willshaw, 1976, 1977; von der Malsburg, 1979; Swindale, 1980; Miller et al., 1989); but without considering the development of the underlying anatomical substrate (the axonal arbors). Miller et al. (1989) have demonstrated that a linear model is sufficient to explain certain features of the development of ocular dominance columns in the absence of changing arbor sizes. It is known, however, that the arbor structure changes during ocular dominance column development and any mechanistic account of how this segregation comes about must therefore explicitly address this issue. As shown in Figure 6, the role of this changing connectivity in the development of ocular dominance columns is accommodated by our present proposal. Assuming that a spatial signal functions as we suggest (see Fig. 6 caption), the ocular dominance columns arise naturally during the ingrowth of fibers serving two simulated retinas.

Although a complete analysis is beyond the scope and intent of this article, the primary constraint on the development of these patterns in this model is the effective cortical distance over which the substance can allow competition for synaptic strength. This distance results from the action of many variables, but is dominated by the substance thresholds for potentiation and depression, the destruction rate of the substance, and the effective axonal arbor sizes (see Appendix 2). During the early ingrowth of the axons into the simulated cortex, the substance production typically does not exhibit a consistent spatial pattern, and the fundamental periodicity of the eye-specific regions is not well defined. The synaptic density increases until a stable average arbor size is reached, after which the interaction distance can stabilize. The effect of eye-specific segregation in this model is complicated primarily by the fact that the arbors are actively growing and thus changing their effective size. In particular, during the initial innervation of the recipient region by the growing axons, we have observed what appear to be shifting wavelengths of the ocular dominance pattern that require the synaptic densities to increase before the system stabilizes.

In these simulations (Fig. 6), the axons from the sensory sheets initially projected with loose topography into the recipient structure. The spatial signaling mechanism also provides a means for both the development and maintenance of topographic mappings (Fig. 7). To demonstrate the development of topography, activity in a simulated retina was modeled in the form of traveling waves of synchronous cell firing (Fig. 7). This kind of activity is one way in which neighborhood relations in the retinal firing patterns could be transmitted to target structures (Mastronarde, 1983a,b; Wong et al., 1990). As shown in Figure 7, only a very loose topographic mapping exists initially between the simulated retina and its target region; that is, a given retinal locus causes depolarization throughout a large portion of the target region (88% of the extent along both the x- and y-axes). This topographic biasing could come about as a result of crude differences in the affinity of nasal and temporal retinal fibers for different regions of the recipient structure (Stahl et al., 1990). As the wave of simulated activity passes repeatedly across the sensory sheet in different directions, the topography progressively refines. This successive refinement of the developing topography illustrates the self-scaling described earlier (Fig. 2*B*). The self-scaling property apparent in this simulation emerges because the postsynaptic responses acquire a diffusive property (see Discussion).

Development of Reciprocal Cortical Connectivity and Neuronal Groups

Most excitatory neurons in the mammalian neocortex project axon collaterals that terminate locally on neighboring cells. In some regions of cortex, these local collaterals may link cells together into functional collectives that have been called neuronal groups (Edelman, 1987). Excitatory cortical neurons can also extend collaterals over greater distances to form reciprocal corticocortical connections both within and between distinct cortical areas. Recent work has shown that axon collaterals originating from cortical neurons in visual areas tend to link cortical domains having similar functional properties (Rockland and Lund, 1982; Gilbert and Wiesel, 1983, 1989; T'so and Gilbert, 1988; Callaway and Katz, 1990, 1991; for anatomical descriptions of intrinsic cortical connections in cat and primate visual cortex, see also Price, 1986; Lund, 1988). The development of these reciprocally connected domains proceeds from an initially even distribution of intrinsic collaterals. This distribution then undergoes a transition to clustered connections that establish reciprocal connectivity among domains receiving correlated functional input (Callaway and Katz, 1990, 1991).

These local and more distant reciprocal connections are known to be a ubiquitous feature of cortical anatomy (Jones et al., 1978; van Essen, 1985; Innocenti, 1986; Zeki and Shipp, 1988). To demonstrate generally how the theory would generate such connections in a cortical area, we simulated activity in local cortical domains and observed the formation and clustering of connections among cortical neurons that received similar functional input. This simulation, illustrated in Figure 8, contains axons originat-

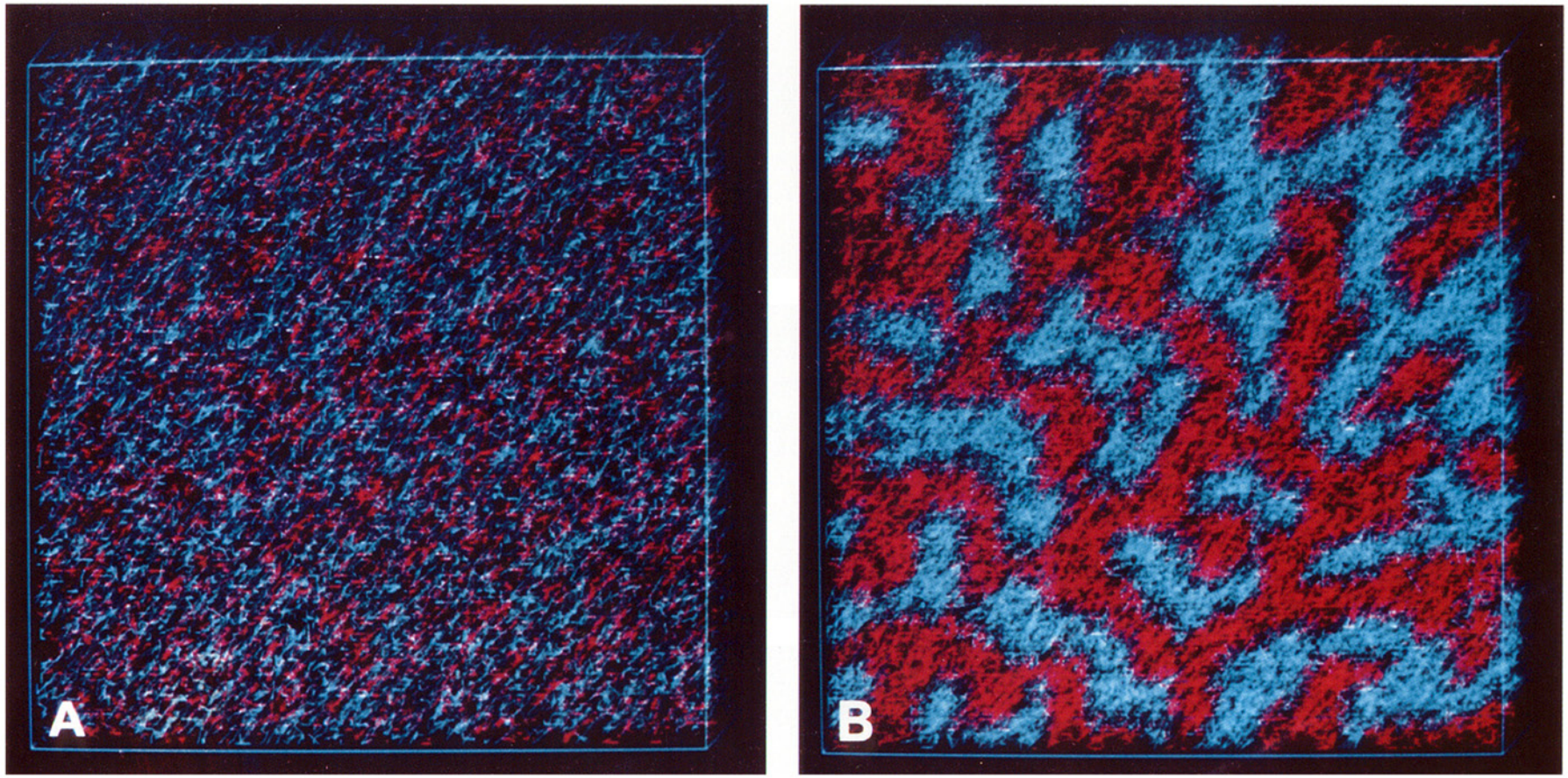

Figure 6. Simulated formation of ocular dominance domains. Two separate 64 × 64 sensory sheets ("retinas") project topographically into a single recipient volume containing 81,920 potential postsynaptic sites with $\sigma_x = \sigma_y = 1.0$ for the initial axonal spread; 40% of these sites are occupied initially ($f = 0.20$ for each retina). Axons from a given retina are similarly colored (*red* and *light blue*). In this simulation, eye-specific firing was accomplished by passing elongated "waves" of activity across each retina over a three- to six-cycle period in different directions. When activity waves passed over one retina, the other retina was quiescent, and visa versa. "Eye-specific" segregation of afferent terminals could also be obtained by activating an entire retina for a three- to six-cycle period while keeping the other quiescent; however, the disruption of topography obviously results from this paradigm. *A* and *B* were taken at cycles 3 and 205, respectively. The fibers from the two retinas segregated, with some overlap at the boundaries between eye-specific domains. Individual arbors either were restricted to a single column or provided input to multiple columns serving one eye. The degree to which arbors innervated multiple columns depended on the resolution or thickness of the waves of activity that defined the neighborhood relationships in the retina. There are approximately six to eight spatial periods of ocular dominance domains along the x- and y-axes. $D = 0.10$; DR = 0.70; IC = 75.0; PR = 20.0; $T_1 = 60.0$, $T_2 = 75.0$, $T_3 = 115.0$; $NC_x = 32$, $NC_y = 32$, $NC_z = 32$; $p_{acc} = 0.4$; $c_{bck} = 0.2$; $n_x = 0.8$–2.0, $n_y = 0.8$–2.0, $n_z = 0.51$–1.01; five layers of synaptic sites each 128 × 128 − NS = 81,920; $\delta = 0.005$.

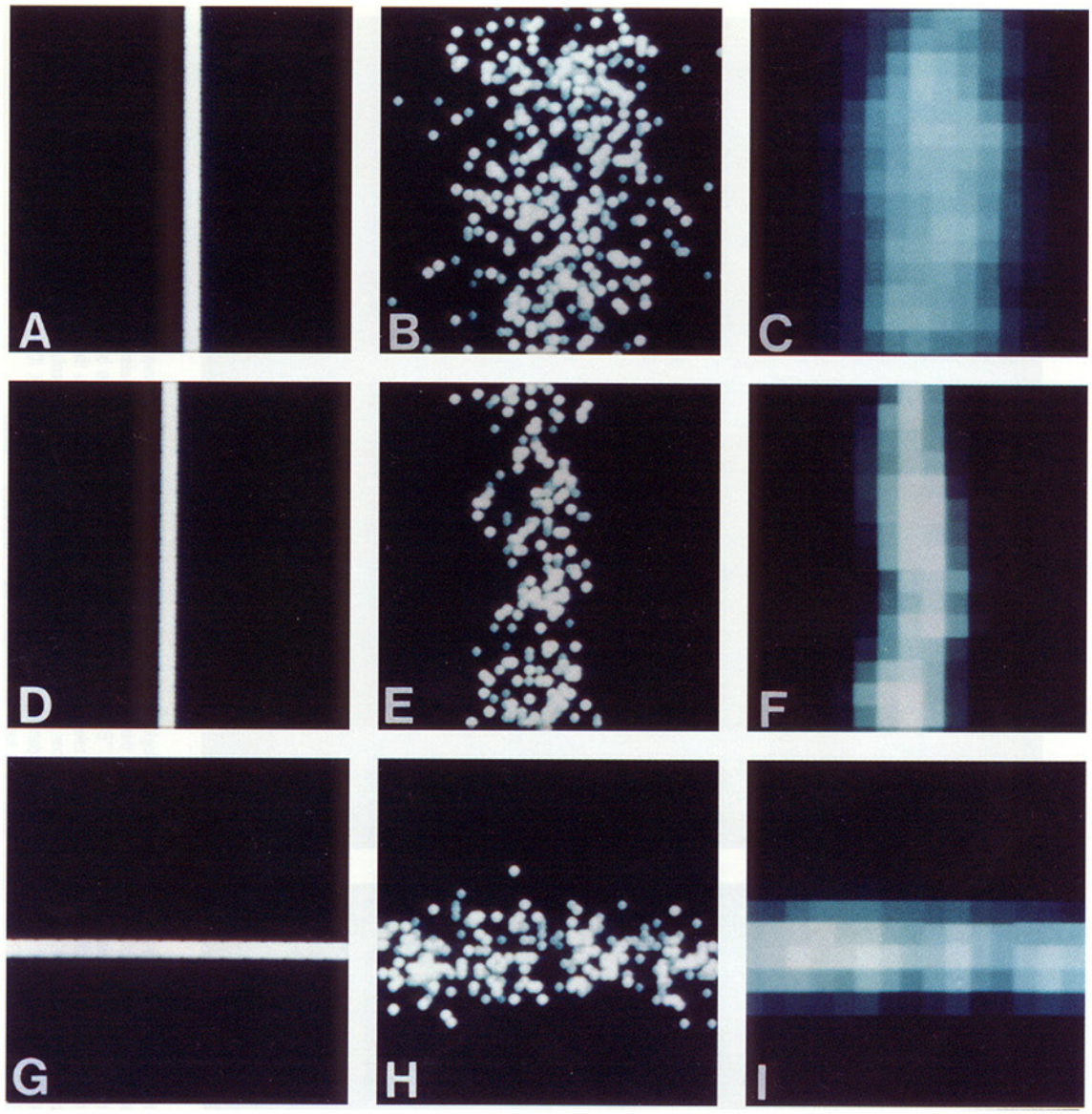

Figure 7. Formation of a topographic mapping from patterned input. A single 64 × 64 sensory sheet ("retina") projected axons into a recipient volume containing 65,536 potential postsynaptic sites; 20% of the sites were occupied initially; 4096 postsynaptic cells distributed throughout the volume extended dendritic arbors into the neuropil in a cylindrically symmetric fashion. The stimulus consisted of traveling "waves" of activity that began in the center of the simulated retina and passed vertically and horizontally across the retina (e.g., *A, D, G*). The waves required approximately 32 cycles to pass across the entire retina. The pattern of firing of postsynaptic cells is illustrated in *B, E,* and *H,* and the concentration of the spatial signal in *C, F,* and *I.* Initial connectivity to the postsynaptic sites was minimally topographic ($\sigma_x = \sigma_y = 10.0$), as is indicated by the *top row* (cycle 5). The *middle row* (*D–F*) and the *bottom row* (*G–I*) were taken at time steps 389 and 405, respectively. The refinement in topography continued until a single retinal cell activated synapses that were distributed across a region that was about 1.5 diffusion compartments along the x- and y-axes. (Firing rates and concentrations are indicated by increasing *brightness* in a 128-level gray scale.) $D = 0.14$; DR = 0.60; IC = 20.0; PR = 4.0; $T_1 = 60.0$, $T_2 = 75.0$, $T_3 = 115.0$; $NC_x = 16$, $NC_y = 16$, $NC_z = 16$; $p_{acc} = 0.2$; $c_{tick} = 0.2$; $n_x = 1.5$, $n_y = 1.5$, $n_z = 0.5$; four layers of synaptic sites, each 128 × 128 − NS = 65,536; $\delta = 0.01$.

ing in a sensory sheet that project with loose topography into the simulated cortex (green fibers). In this simulation, only the active synapses of axons originating in the sensory sheet can generate the spatial signal. The cortical region contains dendrites of both excitatory and inhibitory cells. Although the action of their synaptic contacts differs, both of these simulated cell types project axons into the cortical region that can grow, branch, and make and break synapses in accordance with the covariance of their activity and the spatial signal. Initially, axons of excitatory cells are distributed uniformly throughout the simulated volume, and axons of inhibitory cells arborized locally about their cell of origin.

Random stimulation of four distinct loci in the sensory sheet resulted in the formation of local synaptic domains in the simulated cortex (Fig. 8*A*). After the formation of these domains, the growth of the sensory fibers (green fibers) was halted, but they continued to produce substance at their active synaptic contacts. Continued random firing in each domain led to the formation of groups of locally interconnected cells (Fig. 8*B*). In addition to this effect, those domains whose activity correlates sufficiently become

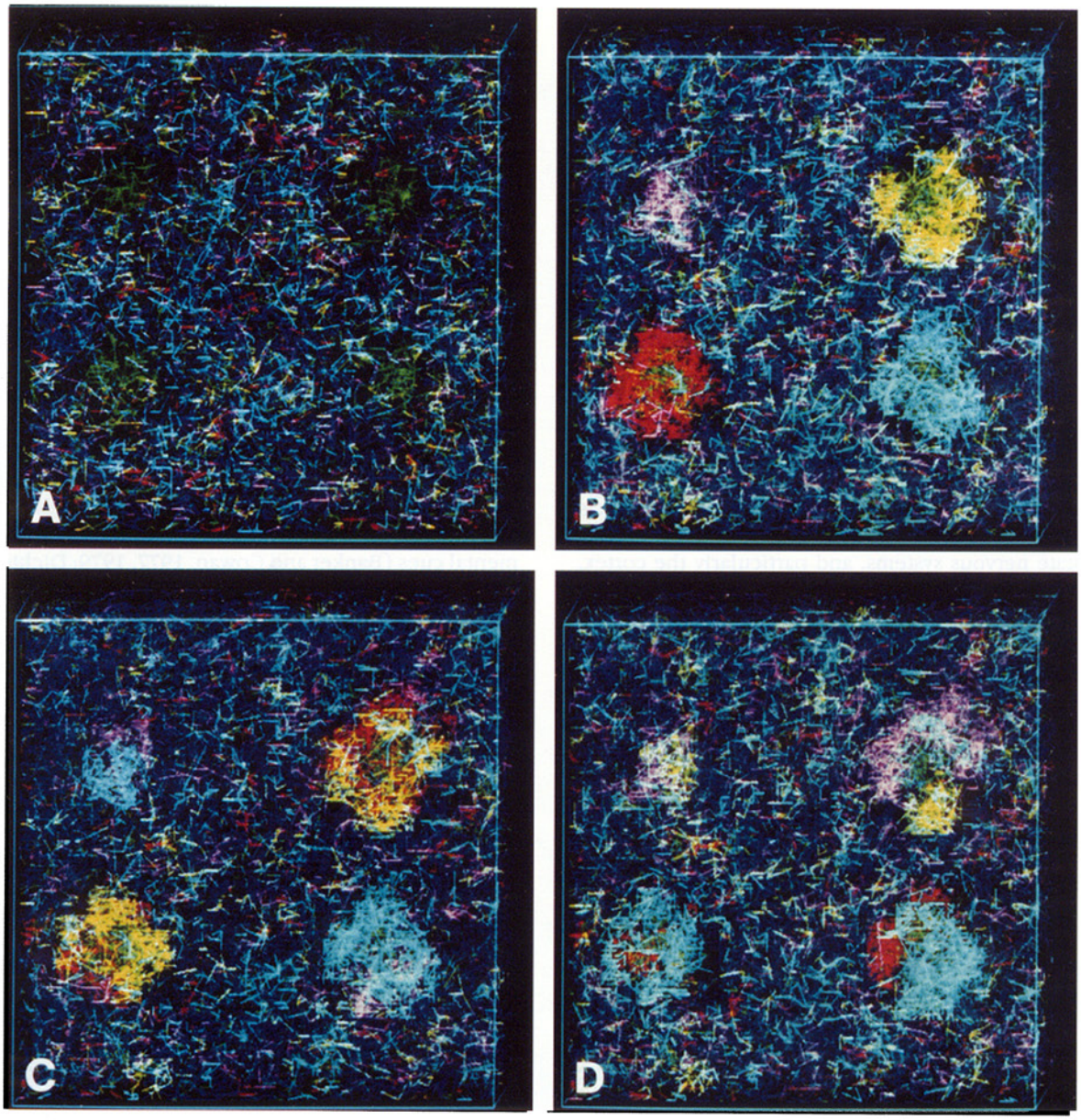

Figure 8. The formation of reciprocal excitatory connectivity. In this simulation, 4096 excitatory cells from a sensory sheet project axons (shown in *green*) topographically into simulated neural tissue ($\sigma_x = \sigma_y = 0.51$). Only synapses from these cells produce the spatial signal, though the strengths of all synapses in the model are modulated in the same manner by this signal. A total of 6400 excitatory cells are located throughout the simulated tissue [cylindrically symmetric dendrites, $\sigma_x = \sigma_y = 1.0$, with synaptic strengths drawn from a narrow Gaussian distribution (mean = 0.3; SD = 0.02)]; these cells also contain axons that initially form synaptic contacts uniformly throughout the volume. The neuropil was divided into four equal-sized parallelepipeds, and the growth of axons arising from excitatory cells in each of these "quarters" was color coded. Top left quarter, *magenta* axons; bottom left quarter, *red* axons; top right quarter, *yellow*; bottom right quarter, *light blue*. *Dark blue* axons originated in a separate sensory sheet and were distributed uniformly, and their activity was drawn from a Gaussian distribution. A total of 6400 inhibitory cells were also present that initially project axons locally. The growth of axons arising from these cells is not shown, but was governed by the same synaptic rules as for excitatory contacts. These inhibitory connections tended to act locally to prevent sustained firing of the excitatory cells as a result of self-excitation. *A*, An initial stage (cycle 10) in neuropil formation. Synchronous bursts of activity in 64 cells at each of four locations in the sensory sheet has induced axonal terminals of these cells to sprout locally and form small afferent domains (*green* fibers). After this initial stage, growth of these axons is stopped. During the simulations, these fibers are active and can generate substance from the postsynaptic dendrites. The *empty areas* are regions occupied primarily by the terminals of the local inhibitory axons. *B*, A later stage (cycle 500). Groups of cells in the sensory sheet that contribute terminals to the four different *green* loci were fired in a randomized order. Because axons formed new synaptic contacts only in those compartments containing a high concentration of spatial signal at the same time that they were active, stable sprouting occurred primarily in localized regions surrounding input axons. *C*, Conditions identical to those in *B*, except that the activity of two pairs of diagonally positioned loci was temporally correlated. After 500 cycles, the *diagonal pairs* of domains had become reciprocally connected. *D*, Conditions identical to those in *B*, except that the activity of the two pairs of horizontally positioned loci was temporally correlated. After 500 cycles, the *horizontal pairs* of domains have become reciprocally connected. $D = 0.13$; DR = 0.60; IC = 80.0; PR = 35.0; $T_1 = 35.0$, $T_2 = 40.0$, $T_3 = 80.0$; $NC_x = 16$, $NC_y = 16$, $NC_z = 16$; $p_{acc} = 0.4$; $c_{dck} = 0.3$; $n_x = 1.8$, $n_y = 1.8$, $n_z = 0.51$; four layers of synaptic sites, each $100 \times 100 -$ NS = 40,000; $\delta = 0.02$.

reciprocally connected (Fig. 8*C,D*). This reciprocal connectivity emerges through the clustering of the intracortical axons in domains with sufficiently correlated activity.

In Figure 8, the formation of locally reentrant connectivity was simulated. However, during the development of the cortex *in vivo*, the growth cones of many cortical neurons also migrate long distances

along fiber tracts that reciprocally connect local and distant cortical regions (van Essen, 1985; Innocenti, 1986; Zeki and Shipp, 1988). As they grow, these axons sprout collaterals that project radially upward into these layers under the control of many influences, which include target-derived growth factors (e.g., O'Leary and Terashima, 1988; Heffner 1990). According to the theory, if these sprouts fire in a temporal pattern that correlates with the local cortical area they enter, they will branch and form synapses there; otherwise, they will not form stable synaptic contacts, and the sprouts would presumably retract or move out of the locale. This would tend to form long-range reciprocal connections among cortical areas on the basis of similar activity patterns.

Discussion

We hypothesize that the development of many aspects of the complex connectivity that characterizes vertebrate nervous systems, and particularly the cortex, may be guided by a short-lived substance or substances made within dendritic processes in response to afferent activity. This substance acts as a diffusive, intercellular signal that transmits temporal correlations among synaptic contacts present within a local volume. Because this mechanism transforms temporal correlation in firing into a diffusible signal that extends throughout a local volume, we have termed this signal a spatial signal. The foregoing theory and simulations demonstrate how the postsynaptic production of such a diffusible signal can translate temporal contiguity of presynaptic activity into spatial contiguity of synaptic contacts.

Covariance in Neural Circuits and Influence of Other Signals

The general notion that the covarying activity of presynaptic and postsynaptic cells mediates synaptic change has been proposed and loosely falls under the "Hebb rule" (Hebb, 1949; von Hayek, 1952). Subsequent variants of this so-called Hebb rule have suggested how the covariance between the activity of pre- and postsynaptic elements that participate in a defined circuit could be stored (Sejnowski, 1977). A more general and statistical "dual rules" model has been proposed to explain how independent short- and long-term synaptic changes in a neuronal network interact in the presence of the extreme variance in the structure of real neural circuits (Finkel and Edelman, 1987). In support of these theoretical considerations, a number of experiments have demonstrated the influence of covarying activity on various kinds of potentiation and depression of different inputs to the same neuron (Lynch et al., 1977; McNaughton et al., 1978; Abraham and Goddard, 1983; Levy and Steward, 1983; Malinow and Miller, 1986; Wigstrom et al., 1986; Stanton and Sejnowski, 1989). However, these proposals have not explained how the structure of neural circuits develops in the first place, how this structure relates to synaptic plasticity, and the nature of the biological mechanism(s) that could mediate these phenomena. These problems are the central concerns of this article.

It is known that synaptic plasticity in the brain can also be affected by such global factors as alertness, attention, and so on. Neurotransmitters released by the diffuse ascending system of neurons housed in the brainstem, for example, may play essential roles in putting CNS neurons into biochemical states necessary to produce or respond to the postulated spatial signal (Pettigrew and Kasamatsu, 1978; Singer, 1985; Bear and Singer, 1986). We point out these interactions only to emphasize our awareness of the complexities of the problem of making specific patterns of synaptic connections and to emphasize that no single mechanism can account for all such patterns.

Interactions with Dendritic Structures

It is known that certain classes of CNS neurons can develop complex dendritic structure characteristic of their region of origin independent of local environmental cues (Banker and Cowan, 1977, 1979; Dichter, 1978; Kriegstein and Dichter, 1983; Banker and Waxman, 1988; Montague and Friedlander, 1989, 1991). These data indicate the existence of strong intrinsic constraints in the elaboration of cell-specific and region-specific dendritic morphology. This intrinsically determined dendritic morphology would act as a regional constraint in developing neuroanatomy. Thus, characteristic regional circuitry could develop in a manner that intimately depended on the activity patterns of the innervating axons and yet still be influenced by the dendritic geometry of cells in the region. In the proposed theory and models, the presynaptic activity patterns do not, however, simply "impress" themselves onto a passive, recipient cortex. Rather, complex statistical relationships between the activity patterns impinging on a region and the dendritic structures characteristic of the region are reflected in the eventual pattern of synapses that forms.

Because the integration of the postsynaptic response occurs in the extracellular space as well as in postsynaptic neurons, this mechanism tends to convolve the afferent activity patterns in both space and time. Thus, neural mappings arise between local volumes of neural tissue as constrained by the source and target cells, rather than by the a priori matching of source and target cells. The mechanism could nevertheless result in a very precise targeting of source and target cells, provided that the afferent activity patterns and postsynaptic dendrites were appropriate for such a case to occur (e.g., dLGN; see Fig. 7).

The Nature of Synaptic "Strength" in the Theory

Once the larger-scale changes in anatomy have slowed or halted, the dynamics of synaptic change in the present model are somewhat similar to those proposed in a model of functional plasticity of single cells in the visual cortex (Bienenstock et al., 1982). This model focused on the development of functional specificity of single cortical neurons and relies upon the covariance of presynaptic activity with a measure of the postsynaptic response. A physiological hypoth-

esis of synaptic modification (Bear et al., 1987) consistent with the model has been proposed.

It should be noted, however, that the dynamics of synaptic change in the present model acquire a variety of extra properties that are critical in building appropriate neuroanatomical connections. These properties arise because the effects of the covariance of presynaptic activity with postsynaptic response in a given volume can be literally transported through the intervening tissue according to a diffusion equation (P. R. Montague, unpublished observations). The similarity of these dynamics to those of Bienenstock et al. (1982) results because the changes in synaptic strength depend upon the covariance of regional substance concentration and the presynaptic activity.

The influence of this covariance is divided between the relative three-dimensional position of a synaptic contact in a local volume and the effective strength of the contact as it mediates transmission from a presynaptic axon to a postsynaptic element. This means that the effective "strength" of any given synapse is not solely a measure of the coupling strength between pre- and postsynaptic elements that participate in a circuit. Rather, it also incorporates the degree to which this synapse contributes to effective depolarization in a local volume in response to different temporal patterns of activity that impinge upon that volume.

The proposal presented here does not exclude other self-consistent explanations that also incorporate a diffusible spatial signal. A phenomenologically equivalent but mechanistically more complicated theory can be constructed if this diffusive link were to be generated presynaptically, both pre- and postsynaptically, or even in local glial cells. Presynaptic production of substance could "label" the surrounding local tissue space according to which afferents had just fired. This would require another signal produced by postsynaptic dendrites that represented the response *elicited* by the presynaptic activity. The conjunction of these two signals could then interact to effect appropriate segregation by stabilizing active synapses in a region that contained suprathreshold levels of both diffusive signals. This type of model requires two diffusive signals to operate effectively.

Candidate Substances and Experimental Tests

The proposed spatial signal is assumed to be released from individual postsynaptic sites in response to neurotransmitter release. How could this come about? One previously suggested candidate for the intradendritic signal required to initiate this process is calcium ions that enter through NMDA receptors (Geiger and Singer, 1986). In the cat cortex, NMDA receptors tend to be present at high levels at those times and places where synaptogenesis or changes in synaptic strength occur (Fox et al., 1989). In addition, it has been shown in some systems that the presence of NMDA blockers can disrupt normal synaptic plasticity and activity-dependent segregation of axonal arbors (Kleinschmidt et al., 1987; Scherer and Udin, 1989; Bear et al., 1990; Cline and Constantine-Paton, 1990).

In an earlier article, we suggested nitric oxide (NO) as one candidate for the spatial signal in an adult nervous system (Gally et al., 1990). NO is produced in a calcium-dependent fashion upon stimulation of NMDA receptors by glutamate or it analogs (Garthwaite et al., 1988, 1989; Bredt and Snyder, 1989), and its synthetic enzyme is located in neurons (Bredt and Snyder, 1990; Bredt et al., 1990). NO is labile, readily diffuses through membranes, and has soluble intracellular enzymes as targets: ADP-ribosylase (Brune and Lapetina, 1989) and soluble guanylate cyclase (Murad et al., 1978; Knowles et al., 1989). Its action would be rapid, would not require the activation of membrane-bound receptors, and would link neural activity to blood flow changes (Gally et al., 1990). Shibuki and Okada (1991) have provided evidence that NO produced by neural activity is required for the induction of synaptic plasticity in the cerebellum. This finding is consistent with our proposal that it may act as a spatial signal.

Similar considerations suggest at least two other potential candidates. Arachidonic acid has been proposed as a diffusible retrograde signal that mediates the induction of long-term potentiation (LTP; Williams et al., 1989). It is released from membranes in a calcium-dependent fashion and is highly lipophilic. Another possibility is hydrogen peroxide. Hydrogen peroxide is a short-lived, diffusible compound that is released from synaptosomal preparations in a calcium-dependent fashion (Zoccarato et al., 1989) and is reported to block the induction of LTP (Colton et al., 1989). Obviously, there are other candidates, and the model does not exclude the possibility that several such substances may act in concert.

In addition to the potential effects of these specific substances, we note that the spatial and temporal scales of changes in substance concentration that are appropriate to guide axonal segregation are also in the range reported for activity-correlated changes in blood flow observed in the visual cortex (Frostig et al., 1990). It is possible that similar biochemical mechanisms underlie both processes, and this possibility is readily accessible to experimental test.

The theory may be tested in a variety of ways; we suggest only a few here: (1) Chronic disruption of the formation or action of potential candidate spatial signals should disrupt developing neuropil. For example, this procedure should disrupt whisker barrel formation, normal somatotopy, and ocular dominance column formation. This action would also be expected from chronic NMDA receptor blockade in any region of cortex. Several effective inhibitors of NO synthase have been reported that could be used in such experiments (Hibbs et al., 1987; Fukuto et al., 1990). Nordihydroguairetic acid (NDGA) is commonly used as an inhibitor of both the formation and the degradation of arachidonate, but its use leads to ambiguous conclusions, because it has also been shown to speed the destruction of NO (Griffith et al., 1984). (2) Chronic inhibition of the firing of cells in the dorsal raphe nuclei (see Fig. 5) will prevent the organization of their terminals into somatotopically

defined units in the somatosensory cortex (see Rhoades et al., 1990). (3) The addition of short-lived substances or activities isolated from the culture medium of stimulated neurons may influence synaptogenesis and axon structure in an *in vitro* system in a manner dependent upon the temporal correlation of the concentration of these substances and activity (Nelson et al., 1989).

Retrograde Signals in Adult Synaptic Plasticity

We have been emphasizing one stage in the development of neuroanatomy. However, NMDA receptors have also been shown to play an essential role in the induction of LTP in the adult nervous system (Bliss and Lynch, 1988; Brown et al., 1988; Nicoll et al., 1988). LTP depends upon correlated presynaptic activity and postsynaptic depolarization and requires an increase in postsynaptic calcium ion concentration for its induction (Dolphin et al., 1982; Collingridge and Bliss, 1987; Davies et al., 1989). LTP has separable pre- and postsynaptic components, and its induction apparently involves some kind of retrograde signal from postsynaptic to presynaptic sites that may be biochemically related to the signal we are proposing (Williams et al., 1989; Bekkers and Stevens, 1990; Malinow and Tsien, 1990; see also Changeux and Danchin, 1976). In particular, a form of "synaptic recruitment" has been observed in cell culture and cortical slices (Bonhoeffer et al., 1989; Kossell et al., 1990), where potentiation of synaptic contacts spreads from the site of induction to active presynaptic terminals in a local region. Although the mechanism mediating this effect is not yet known, the observations are consistent with the production of a diffusible spatial signal.

As a final note, we suggest that the emergence of diffusive mechanisms of the kind hypothesized here may have provided one of the decisive steps in the evolution of nervous systems. Such mechanisms offer a very general means of directing the formation of specific linkages among heterogeneous populations of neurons based on patterns of activity that result from the interaction of a phenotype with its environment.

Appendix 1

If $(s_j(t) - \theta_e) > 0$, that is, if presynaptic terminal j is firing, then three cases arise for changes in $c_{ij}(t)$: (1) $u_i(t) < T_1$ gives depression, (2) $u_i(t) > T_2$ gives potentiation, and (3) $T_1 < u_i(t) < T_2$ gives no change. The third condition implements an intermediate flat zone in the sensitivity of synaptic change to substance concentration. This separates the depression and potentiation components of synaptic strength change. At each time step, c_{ij} changes according to the following difference expressions:

$$c_{ij}(t+1) - c_{ij}(t) = \delta \cdot \rho_w(c_{ij}(t)) \cdot (s_j(t) - \theta_e) \cdot (u_i(t) - T_1),$$

for a depression with no change occurring if $(u_i(t) - T_1) > 0$, and

$$c_{ij}(t+1) - c_{ij}(t) = \delta \cdot \rho_s(c_{ij}(t)) \cdot (s_j(t) - \theta_e) \cdot (u_i(t) - T_2),$$

for potentiation with no change if $(u_i(t) - T_2) \leq 0$.

If $(s_j(t) - \theta_e) \leq 0$, that is, if presynaptic terminal j is not firing, then

$$c_{ij}(t+1) - c_{ij}(t) = \delta \cdot \rho_w(c_{ij}(t)) \cdot (s_j(t) - \theta_e) \cdot (u_i(t) - T_3),$$

for depression with no change if $(u_i(t) - T_3) \leq 0$. The rate of change in the connection strength was scaled by the positive constant δ.

The separate components that caused weakening or strengthening of $c_{ij}(t)$ were weighted by polynomial approximations of sigmoidal functions with $\rho_w(x) = x^4 - 2x^2 + 1$, $\rho_s(x) = -x^4 + 2x^2$. The use of the two weighting functions allows intermediate values of c_{ij} to increase or decrease with equal ease; that is, they allow a "fair" competition for synaptic strengths in an intermediate value range of 0.40–0.60.

In all simulations, the relationship among the concentration thresholds was $T_1 < T_2 < T_3$. The second depression rule (threshold T_3) is effectively equivalent to the first (threshold T_1), but may be biochemically distinct: fibers whose activity does not covary with local activity will tend to fire when the substance concentration is low and will tend not to fire when substance concentration is high. The two depression rules were included for completeness and to approximate better the population effects in an implementation that only allowed a relatively small number of synaptic sites.

Appendix 2

The following remarks may be helpful to readers who desire to reconstruct the simulations.

Generation of Random Numbers and Gaussian Distributions

Uniform deviates were produced by the linear congruential method (see Knuth, 1969). Gaussian distributions were generated using a rapid table look-up method that produces a piecewise rectangular approximation to a Gaussian (Knuth, 1969). Values greater than three times the standard deviation were not generated.

Simulation of the Neuropil

The potential postsynaptic sites were modeled as a series of two-dimensional arrays with fixed dimensions along the x- and y-axes (e.g., 100 × 100 in Fig. 4). These layers could be independently positioned along the z-axis within the simulated tissue space (see Gally et al., 1990, their Fig. 2). The synaptic sites were termed "potential" because they were not functional unless innervated by an axon. The number of diffusion compartments along the x-, y-, and z-axes determined the potential number of synapses per compartment along each of these dimensions. In some cases, in order to maintain an isotropic density of potential synaptic sites, more than one layer of sites was positioned at the same coordinate along the z-axis.

Postsynaptic neurons were introduced separately into the neuropil as a two-dimensional array of units. The x- and y-coordinates of each unit combined with the z-coordinate of the layer determined the exact location of each unit within the simulated tissue space. To define dendritic input, these cell units were assigned input from a specific set of the potential postsynaptic sites located in two-dimensional arrays described above. As described below, this set of inputs also determined the geometry of the dendritic arbors.

Input to the Neuropil from External Sensory Sheets

Topographic input from an external sensory sheet to the neuropil was achieved by assigning a topographically correspondent point on each layer of synaptic sites. For each layer, the connection density of these axons along the x- and y-dimensions varied according to a Gaussian distribution, and the fraction of these sites actually innervated at the beginning of a simulation was one of the parameters required to specify the initial wiring. These parameters include the standard deviations of the Gaussian distributions along the x- and y-axes, and the fraction of occupied sites in the volume potentially covered by the axon.

During the growth of the afferent fibers, a parameter p_{acc} determines the probability that an axonal sprout will actually make a synaptic contact onto an empty postsynaptic site (see Fig. 3). As long as this value remained less than 0.4, its exact value did not greatly influence the overall organization that developed. This is clear when one considers that, if p_{acc} is too large, then a fiber can proceed to branch locally with sufficient speed so that it takes over a small region before the competing activity patterns can eliminate these contacts; that is, for certain patterns of activity in a region, a high value of the acceptance probability allows a fiber to "outrun" locally the effects of the substance fluctuations due to the competing firing patterns in the region.

Determination of Dendritic Geometry of Cells in Recipient Neuropil

In the simulations presented in this article, the neuropil was modeled in two distinct ways. In the first approach, the recipient neuropil was modeled as a three-dimensional array of postsynaptic sites without consideration of the firing in the postsynaptic cells. This type of model represents a simplified version of the segregation of afferents in the thalamus to form retinotopic mappings and barreloid structures. The afferent fibers grow into a region possessing a large number of postsynaptic sites, but these afferents are "blind" to the responses of the postsynaptic cells. This approach essentially ignores the contribution of axons originating in relay cells to local excitatory activity and thus permits the segregation of afferents based solely on the initial connectivity, the number of postsynaptic sites, and the statistics of afferent firing patterns. In this case, the geometry of the dendritic arbors of postsynaptic neurons determines the regions of the neuropil from which each cell takes its input, and this geometry contributes to segregation only by providing a limited number of postsynaptic sites.

To determine the dendritic geometry of the postsynaptic neurons, each neuron is assigned a location in the three-dimensional neuropil. The branches of the dendrites are assigned stochastically at the beginning of the simulation and do not change during the run. Dendritic arbors possessed either spherical or cylindrical symmetry. For cylindrical symmetry, in selecting a synaptic site to provide dendritic input, distances along x- and y-axes centered on the particular cell's location were chosen in accordance with Gaussian distributions with preselected and equal variances. The z-axis distances were drawn from a uniform distribution. For spherical symmetry, distances along x-, y- and z-axes centered on the cell's location were chosen from the same Gaussian distribution.

The number of compartments potentially spanned by a dendritic arbor along a particular dimension is three times the preset standard deviation along that dimension. The standard deviations related to the definition of dendritic arbors are included in the figure legends and are expressed in units of synaptic locations; that is, $\sigma_x = 1.5$ means the standard deviation σ_x is 1.5 synaptic units along the x-axis. After obtaining a distance from the appropriate Gaussian distribution, the distance is rounded to the nearest integer coordinate.

Relationship between Diffusion Equation and Compartmental Simulation

The descriptive equation for the concentration of the signal was given as

$$u_t(\mathbf{x}, t) = D\cdot\nabla^2 u(\mathbf{x}, t) - \kappa\cdot u(\mathbf{x}, t) + p(\mathbf{x}, t).$$

For analytical purposes, the most difficult part of this equation is represented by the substance production term $p(\mathbf{x}, t)$. The production of substance at some location $\mathbf{x}$ depends upon the number of innervated synaptic sites at this location, the distribution of synaptic strengths at this location, and the firing patterns of the innervating afferents. From the point of view of either real or simulated recipient neuropil, these variables are not predictable. In the simulation, the locations $\mathbf{x}$ are quantized by the decomposition of the neuropil into discrete compartments. If the concentration in some compartment is given by u, then $\mathbf{x}$ can be replaced by a compartment index i, and the equation can be written as

$$u_t(i, t) = D\cdot\nabla^2 u(i, t) - \kappa\cdot u(i, t) + p(i, t),$$

which gives

$$u_t(i, t) = D\cdot\nabla^2 u(i, t) - \kappa\cdot u(i, t) + \lambda\cdot \sum_j w_{ij}(t)s_j(t),$$

where the j ranges over the synaptic sites in compartment i, $w_{ij}(t)$ is the weight of site j in compartment i at time t and is 0 if the site is unoccupied. λ is a fixed constant throughout a simulation and represents the production rate of substance (see Table 2 and figure legends for specific values), and $s_j(t)$ is the activity of the afferent at site j and ranges from 0 to

1. Because inhibitory synapses do not produce substance, they are not included in this production term.

In the simulation, diffusion is handled as one-dimensional fluxes between compartments that share a face. As the number of compartments becomes large, this kind of compartmental model can approximate a diffusion equation in three dimensions. In this article, the flux J between adjacent compartments 0 and 1 that share a face of area 1 is computed as

$$J = -D(C_0 - C_1),$$

where C_0 and C_1 are the concentrations in compartments 0 and 1, respectively. The diffusion or coupling constant D is a fixed fraction that is constant throughout a simulation. The limitations on the choice of D in this context are seen by considering a single compartment with concentration C_0 surrounded by its six neighboring compartments. To prevent the occurrence of negative concentrations in a compartment, D cannot exceed the fraction $\frac{1}{6}$. Hence, the following relationship must hold:

$$C_0 - D \cdot \sum_i (C_0 - C_i) \geq 0,$$

where i ranges over neighboring compartments.

The simulations do not represent a computational exploration of the diffusion of particular substances because there is not enough data to model the relevant production rates and lifetimes; however, some relations between the simulation and continuous diffusion can be made. The problem is clear when one considers that the concentration changes within a compartment are felt instantaneously throughout the compartment at each time step. If the compartment were assigned a particular scale, for example, 50 μm along an edge, then this choice immediately sets a minimal size represented by each time step. In the simulations, one can consider, to a very rough approximation, the distance d between compartment centers to be related to the coupling constant D and time t by

$$d^2 \propto D \cdot t.$$

Thus, according to this proportionality, setting any two of these parameters determines the third. For example, the larger the compartment size, the poorer the temporal resolution of the simulation. The lack of information along with the discretization of tissue space does not permit the assessment of absolute spatial and temporal scales that result from the assumptions of the models.

It must be emphasized that, in this article, the simulations were done to display how the proposed model for synaptic change and stabilization can result in appropriate connections and neuroanatomical structures in a manner consistent with a large body of known biological data. In this context, modeling the axons as explicitly as possible represents the central mode of explanation of this article.

Relationships among Parameters in the Simulation

Two of the more important effects in these simulations are the distance over which the substance allows competition for synaptic strength and the effects of crowding. The distance for synaptic strength competition (competition distance) is not sensitive to the coupling or diffusion constant D, but depends primarily upon the afferent firing patterns in a locale, the thresholds for potentiation and depression, and the substance destruction rate.

These relationships are best understood by considering the kinds of effects that tend to be determined by these parameters. The temporal variations in the afferent firing patterns relevant to segregation set the required temporal resolution of the mechanism as it relates to the thresholds and destruction rate. The destruction rate must be large enough to prevent averaging over the relevant fluctuations in afferent activity. In all simulations presented, formation of the neuroanatomical structures could be disrupted by setting the destruction rate too low. The relationships among the thresholds for potentiation and depression were arranged so that synapses of strongly firing fibers ($(s_j(t) - \theta_e) > 0$) were more sensitive to variations in substance concentration than those of weakly firing fibers ($(s_j(t) - \theta_e) \leq 0$; Appendix 1). This allowed weakly firing fibers to grow through regions of the neuropil where the regional activity was out of phase with the weakly firing fibers, but the substance levels were not sufficient to remove completely the transient synaptic contacts of the weakly firing fibers. In any region, strong firing could result in rapid removal of a contact or could "clear out" a region by weakening those synaptic contacts that did not sufficiently covary with regional activity.

In those simulations possessing other fibers with random activity (e.g., Figs. 4, 5, 8), cooperation between coactive synapses was necessary to "clear out" synaptic sites in a region to permit the ingrowth of the coactive fibers. In these cases, synaptic contacts by fibers that fired weakly and randomly were weakened and broken, thus increasing the likelihood that the cooperating fibers would grow into and branch throughout the region. This effect accounted for the "squeezing" of the uncorrelated fibers into the septa between the forming or reorganizing barreloids.

Notes

See the cover of the previous issue for a computer simulation of the emergence of reciprocal excitatory connectivity in a sheet of sensory cells.

We appreciate the helpful comments of Drs. B. A. Cunningham, K. C. Crossin, G. N. Reeke Jr., O. Sporns, and G. Tononi. This work was carried out as part of the Institute Fellows in Theoretical Neurobiology program at The Neurosciences Institute, which is supported by the Neurosciences Research Foundation. We are particularly grateful to Fidia, S.p.A. and the Office of Naval Research for grants in partial support of this research.

Dr. Edelman is director of The Neurosciences Institute and Vincent Astor Professor at the Rockefeller University, New York, NY 10021. Dr. Montague is now at The Neurobiology Research Center, Volker Hall, UAB Station, Birmingham, AL 35294.

Address correspondence to Dr. Edelman, The Neurosciences Institute, 1230 York Ave., New York, NY 10021.

References

Abraham WC, Goddard GV (1983) Asymmetric relationships between homosynaptic long-term potentiation and heterosynaptic long-term depression. Nature 305:717–719.

Artola A, Singer W (1987) Long-term potentiation and NMDA receptors in rat visual cortex. Nature 330:649–652.
Artola A, Singer W (1990) The involvement of *N*-methyl-D-aspartate receptors in the induction and maintenance of long-term potentiation in rat visual cortex. Eur J Neurosci 2:254–269.
Artola A, Brocher S, Singer W (1990) Different voltage-dependent thresholds for inducing long-term depression and long-term potentiation in slices of rat visual cortex. Nature 347:69–72.
Banker GA, Cowan WM (1977) Rat hippocampal neurons in dispersed cell culture. Brain Res 126:397–425.
Banker GA, Cowan WM (1979) Some further observations on hippocampal neurons in dispersed cell culture. J Comp Neurol 187:469–494.
Banker GA, Waxman AB (1988) Hippocampal neurons generate natural shapes in cell cultures. In: Intrinsic determinants of neuronal form and function (Lasek RJ, Black MM, eds), pp 61–82. New York: Liss.
Bear MF, Singer W (1986) Modulation of visual cortical plasticity by acetylcholine and noradrenaline. Nature 320: 172–175.
Bear MF, Cooper LN, Ebner FF (1987) A physiological basis for a theory of synapse modification. Science 237:42–48.
Bear MF, Kleinschmidt A, Gu Q, Singer W (1990) Disruption of experience-dependent synaptic modifications in striate cortex by infusion of an NMDA receptor antagonist. J Neurosci 10:909–925.
Bekkers JM, Stevens CF (1990) Presynaptic mechanism for long-term potentiation in the hippocampus. Nature 346: 724–729.
Belford GR, Killackey HP (1979) Vibrissae representation in subcortical trigeminal centers of the neonatal rat. J Comp Neurol 183:305–322.
Bienenstock EL, Cooper LN, Munro PW (1982) Theory for the development of neuron selectivity: orientation specificity and binocular interaction in visual cortex. J Neurosci 2:32–48.
Bliss TVP, Lynch MA (1988) Long term potentiation of synaptic transmission in the hippocampus: properties and mechanisms. In: Long-term potentiation: from biophysics to behavior (Landfield PW, Deadwyler SA, eds), pp 3–72. New York: Liss.
Bonhoeffer F, Huff J (1985) Position-dependent properties of retinal axons and their growth cones. Nature 315:409–410.
Bonhoeffer T, Staiger V, Aersen A (1989) Synaptic plasticity in rat hippocampal slice cultures: local "Hebbian" conjunction of pre- and postsynaptic stimulation leads to distributed synaptic enhancement. Proc Natl Acad Sci USA 86:8113–8117.
Bredt DS, Snyder S (1989) Nitric oxide mediates glutamate-linked enhancement of cGMP levels in the cerebellum. Proc Natl Acad Sci USA 86:9030–9033.
Bredt DS, Snyder S (1990) Isolation of nitric oxide synthetase, a calmodulin-requiring enzyme. Proc. Natl Acad Sci USA 87:682–685.
Bredt DS, Hwang PM, Snyder SH (1990) Localization of nitric oxide synthase indicating a neural role for nitric oxide. Nature 347:768–770.
Brown TH, Chapman PF, Kairiss EW, Keenan CL (1988) Long-term synaptic potentiation. Science 242:724–728.
Brune B, Lapetina EG (1989) Activation of a cytosolic ADP-ribosyltransferase by nitric oxide–generating agents. J Biol Chem 264:8455–8458.
Callaway EM, Katz LC (1990) Emergence and refinement of clustered horizontal connections in cat striate cortex. J Neurosci 10:1134–1153.
Callaway EM, Katz LC (1991) Effects of binocular deprivation on the development of clustered horizontal connections in cat striate cortex. Proc Natl Acad Sci USA 88: 745–749.
Changeux JP, Danchin A (1976) Selective stabilization of developing synapses as a mechanism for the specification of neuronal networks. Nature 264:705–712.
Changeux JP, Courrege P, Danchin A (1973) A theory of epigenesis of neuronal networks by selective stabilization of synapses. Proc Natl Acad Sci USA 70:2974–2978.
Clark RM, Allard T, Jenkins WM, Merzenich MM (1988) Receptive fields in the body surface map in adult cortex defined by temporally correlated inputs. Nature 332:444–446.
Cline HT, Constantine-Paton M (1990) NMDA antagonists disrupt the retinotectal topographic map. Neuron 3:413–426.
Cline HT, Debski EA, Constantine-Paton M (1987) *N*-methyl-D-aspartate receptor antagonist desegregates eye-specific stripes. Proc Natl Acad Sci USA 84:4342–4345.
Collingridge GL, Bliss TVP (1987) NMDA receptors—their role in long-term potentiation. Trends Neurosci 10:288–293.
Colton CA, Fagni L, Gilbert D (1989) The action of hydrogen peroxide on paired pulse and long-term potentiation in the hippocampus. Free Radical Biol Med 7:3–8.
Constantine-Paton M, Law RI (1978) Eye-specific termination bands in tecta of three-eyed frogs. Science 202: 639–641.
Constantine-Paton M, Cline HT, Debski E (1990) Patterned activity, synaptic convergence, and the NMDA receptor in developing visual pathways. Annu Rev Neurosci 13: 129–154.
Cook JE (1987) A sharp retinal image increases the topographic precision of the goldfish retinotectal projection during optic nerve regeneration in stroboscopic light. Exp Brain Res 68:319–328.
Cowan WM (1978) Aspects of neural development. In: International reviews of physiology (Porter R, ed), pp 149–208. Baltimore: University Park.
Crank J (1955) The mathematics of diffusion. Oxford: Oxford UP.
Cussler EL (1984) Diffusion. Cambridge: Cambridge UP.
Davies SN, Lester RAJ, Reymann KG, Collingridge GL (1989) Temporally distinct pre- and post-synaptic mechanisms maintain long-term potentiation. Nature 338:500–503.
Dawson DR, Killackey HP (1987) The organization and mutability of the forepaw and hindpaw representations in the somatosensory cortex of the neonatal rat. J Comp Neurol 256:246–256.
Dichter MA (1978) Rat cortical neurons in cell culture: culture methods, cell morphology, electrophysiology, and synapse formation. Brain Res 149:279–293.
Dodd J, Jessel T (1988) Axon guidance and patterning of neuronal projections in vertebrates. Science 242:692–699.
Dolphin AC, Errington ML, Bliss TVP (1982) Long-term potentiation of the perforant path *in vivo* is associated with increased glutamate release. Nature 297:496–498.
Dubin MW, Stark LA, Archer SM (1986) A role for action-potential activity in the development of neuronal connections in the kitten retinogeniculate pathway. J Neurosci 6:1021–1036.
Durham D, Woolsey TA (1984) Effects of neonatal whisker lesion on mouse central trigeminal pathways. J Comp Neurol 223:424–447.
Edelman GM (1987) Neural Darwinism. New York: Basic.
Finkel LH, Edelman GM (1987) Population rules for synapses in networks. In: Synaptic function (Edelman GM, Gall WE, Cowan WM, eds), pp 711–757. New York: Wiley-Interscience.
Fox K, Sato H, Daw N (1989) The location and function of NMDA receptors in cat and kitten visual cortex. J Neurosci 9:2443–2454.
Fregnac Y, Imbert M (1984) Development of neuronal selectivity in the primary visual cortex of the cat. Physiol Rev 64:325–434.
Fregnac Y, Schulz D, Thorpe S, Bienenstock E (1988) A cellular analogue of visual cortical plasticity. Nature 333: 367–370.
Friedlander MJ, Martin KAC (1989) Development of

Y-axon innervation of cortical area 18 in the cat. J Physiol (Lond) 416:183–213.
Frost DO, Metin C (1985) Induction of functional retinal projections to the somatosensory system. Nature 317:162–164.
Frostig RD, Lieke ED, Ts'o DY, Grinvald A (1990) Cortical functional architecture and local coupling between neuronal activity and the microcirculation revealed by *in vivo* high-resolution optical imaging of intrinsic signals. Proc Natl Acad Sci USA 87:6082–6086.
Fukuto JM, Wood KS, Byrns RE, Ignarro LJ (1990) N^G-amino-L-arginine: a new potent antagonist of L-arginine–mediated endothelium-dependent relaxation. Biochem Biophys Res Commun 168:458–465.
Gally JA, Montague PR, Reeke GN, Edelman GM (1990) The NO hypothesis: possible effects of a rapidly diffusible substance in neural development and function. Proc Natl Acad Sci USA 87:3547–3551.
Garraghty PE, Shatz CJ, Sur MJ (1988) Prenatal disruption of binocular interactions creates novel lamination in the cat's lateral geniculate nucleus. Visual Neurosci 1:93–102.
Garthwaite J, Charles SL, and Chess-Williams R (1988) Endothelium-derived relaxing factor release on activation of NMDA receptors suggests role as intercellular messenger in the brain. Nature 336:385–388.
Garthwaite J, Garthwaite G, Palmer RMJ, Moncada S (1989) NMDA receptor activation induces nitric oxide synthesis from arginine in rat brain slices. Eur J Pharmacol 172: 413–416.
Geiger H, Singer W (1986) A possible role of Ca^{++} currents in developmental plasticity. Exp Brain Res 14:256–270.
Gilbert CD, Wiesel TN (1983) Clustered intrinsic connections in the cat visual cortex. J Neurosci 3:1116–1133.
Gilbert CD, Wiesel TN (1989) Columnar specificity of intrinsic horizontal and corticocortical connections in cat visual cortex. J Neurosci 9:2432–2442.
Goldman RS, Chavez-Noriega LE, Stevens CF (1990) Failure to reverse long-term potentiation by coupling sustained presynaptic activity and *N*-methyl-D-aspartate receptor blockade. Proc Natl Acad Sci USA 87:7165–7169.
Griffith TM, Edwards DH, Lewis MJ, Newby AC, Henderson AH (1984) The nature of endothelium-derived vascular relaxant factor. Nature 308:645–647.
Harris WA (1989) Local positional cues in the neuroepithelium guide retinal axons in embryonic *Xenopus* brain. Nature 339:218–221.
Harris WA, Holt CE (1990) Early events in the embryogenesis of the vertebrate visual system: cellular determination and pathfinding. Annu Rev Neurosci 13:155–169.
Hebb DO (1949) The organization of behavior. New York: Wiley.
Heffner CD, Lumsden AGS, O'Leary DDM (1990) Target control of collateral extension and directional growth in the mammalian brain. Science 247:217–220.
Hibbs HB, Vavrin Z, Taintor R (1987) L-Arginine is required for expression of the activated macrophage effector mechanism causing selective metabolic inhibition in target cells. J Immunol 138:550–556.
Hubel DH, Wiesel TN (1965) Binocular interactions in striate cortex of kittens reared with artificial squint. J Neurophysiol 28:1041–1059.
Hubel DH, Wiesel TN (1970) The period of susceptibility to the physiological effects of unilateral eye closure in kittens. J Physiol (Lond) 206:419–436.
Hubel DH, Wiesel TN, LeVay S (1977) Plasticity of ocular dominance columns in monkey striate cortex. Philos Trans R Soc Lond [Biol] 278:377–409.
Innocenti GM (1986) Cerebral cortical organization of callosal connections in the cerebral cortex. In: Cerebral cortex, Vol 5 (Jones EG, Peters A, eds), pp 291–354. New York: Plenum.
Jacobson M (1978) Developmental neurobiology. New York: Plenum.
Jensen KF, Killackey HP (1987a) Terminal arbors of axons projecting to the somatosensory cortex of the adult rat. I. The normal morphology of specific thalamocortical afferents. J Neurosci 7:3529–3543.
Jensen KF, Killackey HP (1987b) Terminal arbors of axons projecting to the somatosensory cortex of the adult rat. II. The altered morphology of thalamocortical afferents following neonatal infraorbital nerve cut. J Neurosci 7: 3544–3553.
Jones EG (1985) The thalamus. New York: Plenum.
Jones EG, Coulter JD, Hendry SHC (1978) Intracortical connectivity of architectonic fields in the somatic sensory, motor, and parietal cortex of monkeys. J Comp Neurol 181:291–348.
Kaas JH, Krubitzer LA, Chino YM, Langston AL, Polley EH, Blair N (1990) Reorganization of retinotopic cortical maps in adult mammals after lesions of the retina. Science 248:227–229.
Killackey HP (1973) Anatomical evidence for cortical subdivisions based on vertically discrete thalamic projections from the ventral posterior nucleus to cortical barrels in the rat. Brain Res 51:326–331.
Killackey HP, Belford GR (1979) The formation of afferent patterns in the somatosensory cortex of the neonatal rat. J Comp Neurol 183:285–304.
Kleinschmidt A, Bear MF, Singer W (1987) Blockade of NMDA receptors disrupts experience-dependent plasticity of kitten striate cortex. Science 238:355–358.
Knowles RG, Palacios M, Palmer J, Moncada S (1989) Formation of nitric oxide from L-arginine in the central nervous system: a transduction mechanism for stimulation of the soluble guanylate cyclase. Proc Natl Acad Sci USA 86:5159–5162.
Knuth DE (1969) The art of computer programming, Vol 2, Seminumerical algorithms. Reading, MA: Addison-Wesley.
Kossell A, Bonhoeffer T, Bolz J (1990) Non-Hebbian synapses in rat visual cortex. Neuro-Report 1:115–118.
Kriegstein AR, Dichter MA (1983) Morphological classification of rat cortical neurons in culture. J Neurosci 3: 1634–1647.
LeVay S, Wiesel TN, Hubel DH (1980) The development of ocular dominance columns in normal and visually deprived monkeys. J Comp Neurol 191:1–51.
Levy WB, Steward O (1983) Temporal contiguity requirements for long term associative potentiation/depression in the hippocampus. Neuroscience 8:791–797.
Lund JS (1988) Anatomical organization of macaque monkey striate visual cortex. Annu Rev Neurosci 11:253–288.
Lynch GS, Dunwiddie T, Gribkoff V (1977) Heterosynaptic depression: a postsynaptic correlate of long-term potentiation. Nature 266:737–739.
Malinow R, Miller JP (1986) Postsynaptic hyperpolarization during conditioning reversibly blocks induction of long term potentiation. Nature 320:529–530.
Malinow R, Tsien RW (1990) Presynaptic enhancement shown by whole-cell recordings of long-term potentiation in hippocampal slices. Nature 346:177–180.
Mastronarde DN (1983a) Correlated firing of cat retinal ganglion cells. I. Spontaneously active inputs to X- and Y-cells. J Neurophysiol 49:303–324.
Mastronarde DN (1983b) Correlated firing of cat retinal ganglion cells. II. Responses of X- and Y-cells to single quantal events. J Neurophysiol 49:325–349.
McNaughton BL, Douglas RM, Goddard GV (1978) Synaptic enhancements in fascia dentata: cooperativity among coactive afferents. Brain Res 157:277–293.
Merzenich MM, Jenkins WM, Middlebrooks JC (1985) Observations and hypotheses on special organizational features of the central auditory nervous system. In: Dynamic aspects of neocortical function (Edelman GM, Gall WE, Cowan WM, eds), pp 633–695. New York: Wiley.
Metin C, Frost DO (1989) Visual responses of neurons in somatosensory cortex of hamsters with experimentally induced projections to somatosensory thalamus. Proc Natl Acad Sci USA 86:357–361.
Meyer RL (1982) Tetrodotoxin blocks the formation of

ocular dominance columns in goldfish. Science 218:589–591.
Miller KD, Keller JB, Stryker MP (1989) Ocular dominance column development: analysis and simulation. Science 245:605–615.
Montague PR, Friedlander MJ (1989) Expression of an intrinsic growth strategy by mammalian retinal neurons. Proc Natl Acad Sci USA 86:7223–7229.
Montague PR, Friedlander MJ (1991) Morphogenesis and territorial coverage by isolated mammalian retinal ganglion cells. J Neurosci 11:1440–1457.
Murad F, Mittal CK, Arnold WP, Katsuki S, Kimura H (1978) Guanylate cyclase: activation by azide, nitro compounds, nitric oxide, and hydroxyl radical and inhibition by hemoglobin and myoglobin. Adv Cyclic Nucleotide Res 9: 145–158.
Nelson PG, Yu C, Fields RD, Neale EA (1989) Synaptic connections *in vitro*: modulation of number and efficacy by electrical activity. Science 244:585–587.
Nicoll RA, Kauer JA, Malenka RC (1988) The current excitement in long-term potentiation. Neuron 1:97–103.
O'Leary DDM, Terashima T (1988) Cortical axons branch to multiple subcortical targets by interstitial axon budding: implications for target recognition and "waiting periods." Neuron 4:901–910.
Pearson JC, Finkel LH, Edelman GM (1987) Plasticity in the organization of adult cerebral cortical maps: a computer simulation based on neuronal group selection. J Neurosci 7:4209–4223.
Pettigrew JD (1974) The effects of visual experience on the development of stimulus specificity by kitten cortical neurons. J Physiol (Lond) 237:49–74.
Pettigrew JD, Kasamatsu T (1978) Local perfusion of noradrenaline maintains visual cortical plasticity. Nature 271: 761–763.
Price DJ (1986) The postnatal development of clustered intrinsic connections in area 18 of the visual cortex in kittens. Dev Brain Res 24:31–38.
Purves D, Lichtman JW (1985) Principles of neural development. Sunderland, MA: Sinauer.
Rakic P (1976) Prenatal genesis of connections subserving ocular dominance in the rhesus monkey. Nature 261:467–471.
Rakic P (1981) Development of visual centers in the primate brain depends on binocular competition before birth. Science 214:928–931.
Rauschecker JP, Singer W (1979) Changes in the circuitry of the kitten's visual cortex are gated by postsynaptic activity. Nature 280:58–60.
Reeke GN, Finkel LH, Sporns O, Edelman, GM (1990) Synthetic neural modeling: A multilevel approach to the analysis of brain complexity. In: Signal and sense (Edelman GM, Gall WE, Cowan WM, eds), pp 607–707. New York: Wiley-Liss.
Reh TA, Constantine-Paton M (1985) Eye-specific segregation requires neural activity in three-eyed *Rana pipiens*. J Neurosci 5:1132–1143.
Reiter HO, Stryker MP (1988) Neural plasticity without postsynaptic action potentials: less active inputs become dominant when kitten visual cortical cells are pharmacologically inhibited. Proc Natl Acad Sci USA 85:3623–3627.
Reiter HO, Waitzman DM, Stryker MP (1986) Cortical activity blockade prevents ocular dominance plasticity in the kitten visual cortex. Exp Brain Res 65:182–188.
Rhoades RW, Bennet-Clark CA, Chiaia NL, Fletcher AW, Macdonald GJ, Haring JH, Jacquin MF (1990) Development and lesion induced reorganization of the cortical representation of the rat's body surface as revealed by immunocytochemistry for serotonin. J Comp Neurol 293: 190–207.
Rockland KS, Lund JS (1982) Widespread periodic intrinsic connections in the tree shrew visual cortex. Science 215:1532–1534.
Scherer WJ, Udin SB (1989) *N*-methyl-D-aspartate antagonists prevent interaction of binocular maps in *Xenopus* tectum. J Neurosci 9:3837–3843.
Schmidt JT (1990) Long-term potentiation and activity-dependent retinotopic sharpening in the regenerating retinotectal projection of goldfish: common sensitive period and sensitivity to NMDA blockers. J Neurosci 10: 233–246.
Schmidt JT, Eisele LE (1985) Stroboscopic illumination and dark rearing block the sharpening of the retinotectal map in goldfish. Neuroscience 14:535–546.
Sejnowski TJ (1977) Storing covariance with nonlinearly interacting neurons. J Math Biol 4:303–321.
Shatz CJ, Stryker MP (1978) Ocular dominance in layer IV of the cat's visual cortex and the effects of monocular deprivation. J Physiol (Lond) 281:267–283.
Shatz CJ, Stryker MP (1988) Tetrodotoxin infusion prevents the formation of eye-specific layers during prenatal development of the cat's retinogeniculate projection. Science 242:87–89.
Sherman SM, Spear PD (1982) Organization of visual pathways in normal and visually deprived cats. Physiol Rev 62:740–855.
Shibuki K, Okada D (1991) Endogenous nitric oxide release required for long-term synaptic depression in the cerebellum. Nature 349:326–328.
Singer W (1985) Central control of developmental plasticity in the mammalian visual cortex. Vision Res 25:389–396.
Sperry RW (1943a) Effect of 180-degree rotation of the retinal field on visuomotor coordination. J Exp Zool 92: 263–279.
Sperry RW (1943b) Visuomotor coordination in the newt (*Triturus viridescens*) after regeneration of the optic nerve. J Comp Neurol 79:33–55.
Sretavan DW (1990) Specific routing of retinal ganglion cell axons at the mammalian optic chiasm during embryonic development. J Neurosci 10:1995–2007.
Sretavan DW, Shatz CJ (1986) Prenatal development of retinal ganglion cell axons: segregation into eye-specific layers within the cat's lateral geniculate nucleus. J Neurosci 6:234–251.
Sretavan DW, Shatz CJ, Stryker MP (1988) Modification of retinal ganglion cell axon morphology by prenatal infusion of tetrodotoxin. Nature 336:468–471.
Stahl B, Muller B, von Boxberg Y, Cox EC, Bonhoeffer F (1990) Biochemical characterization of a putative axonal guidance molecule of the chick visual system. Neuron 5:735–743.
Stanton PK, Sejnowski TJ (1989) Associative long-term depression in the hippocampus induced by Hebbian covariance. Nature 339:215.
Stryker MP, Harris WA (1986) Binocular impulse blockade prevents the formation of ocular dominance columns in cat visual cortex. J Neurosci 6:2117–2133.
Stuermer CAO (1988) Retinotopic organization of the developing retinotectal projection in the zebrafish embryo. J Neurosci 8:4513–4530.
Sur M, Garraghty PA, Roe AW (1988) Experimentally induced visual projections into auditory thalamus and cortex. Science 242:1437–1441.
Swindale NV (1980) A model for the formation of ocular dominance stripes. Proc R Soc Lond [Biol] 208:243–264.
Swindale NV (1988) Role of visual experience in promoting segregation of eye dominance patches in the visual cortex of the cat. J Comp Neurol 267:472–488.
T'so DY, Gilbert CD (1988) The organization of chromatic and spatial interactions in the primate striate cortex. J Neurosci 8:1712–1727.
Udin SB, Fawcett JW (1988) Formation of topographic maps. Annu Rev Neurosci 11:289–328.
Udin SB, Scherer WJ (1990) Restoration of the plasticity of binocular maps by NMDA after the critical period in *Xenopus*. Science 249:669–672.
Van der Loos H, Dorfl J (1978) Does the skin tell the somatosensory cortex how to construct a map of the periphery? Neurosci Lett 7:23–30.

Van der Loos H, Woolsey TA (1973) Somatosensory cortex: structural alterations following early injury to sense organs. Science 129:395–398.
Van Essen DC (1985) Functional organization of primate visual system. In: Cerebral cortex, Vol 3 (Peters A, Jones EG, eds), pp 259–329. New York: Plenum.
von der Malsburg C (1979) Development of ocularity domains and growth behavior of axon terminals. Biol Cybern 32:49–62.
von der Malsburg C, Willshaw DJ (1976) A mechanism for producing continuous neural mappings: ocularity dominance stripes and ordered retinotectal projections. Exp Brain Res [Suppl] 1:463–469.
von der Malsburg C, Willshaw DJ (1977) How to label nerve cells so they can interconnect in an ordered fashion. Proc Natl Acad Sci USA 74:5176–5178.
von Hayek FA (1952) The sensory order: an inquiry into the foundations of theoretical psychology. Chicago: University of Chicago Press.
White G, Levy WB, Steward O (1988) Evidence that associative interactions between synapses during the induction of long-term potentiation occur within local dendritic domains. Proc Natl Acad Sci USA 85:2368–2372.
White G, Levy WB, Steward O (1990) Spatial overlap between populations of synapses determines the extent of their associative interaction during the induction of long-term potentiation and depression. J Neurophysiol 64: 1186–1198.
Wigstrom H, Gustaffson B, Huang YY (1986) Hippocampal long-lasting potentiation is induced by pairing single afferent volleys with intracellularly injected depolarizing current pulses. Acta Physiol Scand 126:317–319.
Williams JH, Errington ML, Lynch MA, Bliss TVP (1989) Arachidonic acid induces a long-term activity-dependent enhancement of synaptic transmission in the hippocampus. Nature 341:739–742.
Wong ROL, Meister M, Baylor DA, Shatz CJ (1990) Locally correlated spontaneous activity of neurons in the developing mammalian retina. Soc Neurosci Abstr 16:1128.
Woolsey TA, Wann JR (1976) Areal changes in mouse cortical barrels following vibrissal damage at different postnatal ages. J Comp Neurol 170:53–66.
Woolsey TA, Dierker ML, Wann DF (1975) Mouse SmI cortex: qualitative and quantitative classification of Golgi-impregnated neurons. Proc Natl Acad Sci USA 72:2165–2169.
Zeki S, Shipp S (1988) The functional logic of cortical connections. Nature 335:311–317.
Zoccarato F, Deana R, Cavallini L, Alexandre A (1989) Generation of hydrogen peroxide by cerebral-cortex synaptosomes. Eur J Biochem 180:473–478.